

Received September 18, 2021, accepted October 7, 2021, date of publication October 13, 2021, date of current version October 25, 2021.

Digital Object Identifier 10.1109/ACCESS.2021.3119561

Deep-Learning for Radar: A Survey

ZHE GENG^{ID}, (Member, IEEE), HE YAN^{ID}, JINDONG ZHANG^{ID}, AND DAIYIN ZHU^{ID}

College of Electronic and Information Engineering, Nanjing University of Aeronautics and Astronautics (NUAA), Nanjing 210016, China

Corresponding author: Zhe Geng (zhe.geng@ieee.org)

This work was supported in part by the Fundamental Research Funds for the Central Universities under Grant 1004-XZA20014, in part by the Natural Science Foundation from Jiangsu Province under Grant BK20200420, and in part by the Research Funds for New Faculty of NUAA under Grant 1004-YAH19111.

ABSTRACT A comprehensive and well-structured review on the application of deep learning (DL) based algorithms, such as convolutional neural networks (CNN) and long-short term memory (LSTM), in radar signal processing is given. The following DL application areas are covered: i) radar waveform and antenna array design; ii) passive or low probability of interception (LPI) radar waveform recognition; iii) automatic target recognition (ATR) based on high range resolution profiles (HRRPs), Doppler signatures, and synthetic aperture radar (SAR) images; and iv) radar jamming/clutter recognition and suppression. Although DL is unanimously praised as the ultimate solution to many bottleneck problems in most of existing works on similar topics, both the positive and the negative sides of stories about DL are checked in this work. Specifically, two limiting factors of the real-life performance of deep neural networks (DNNs), limited training samples and adversarial examples, are thoroughly examined. By investigating the relationship between the DL-based algorithms proposed in various papers and linking them together to form a full picture, this work serves as a valuable source for researchers who are seeking potential research opportunities in this promising research field.

INDEX TERMS Deep-learning, radar waveform recognition, synthetic aperture radar (SAR), automatic target recognition (ATR), adversarial examples, jamming recognition.

I. INTRODUCTION

In recent years, top researchers around the world have been increasingly resorting to deep learning (DL) based algorithms to solve bottle-neck problems in the field of radar signal processing [1], [2]. The amount of publications on “deep learning for radar” have been increasing rapidly. To illustrate radar engineers’ soaring interests in DL, the number of publications on the topic of “deep learning for radar” from 2016 to 2020 are plotted in **Fig. 1** (IEEE Xplore database).

Specifically, a comprehensive survey of machine learning algorithms applied to radar signal processing is given in [3], where six aspects are considered: i) radar radiation sources classification and recognition; ii) radar image processing; iii) anti-jamming & interference mitigation; iv) application of machine learning in research fields other than i) - iv); v) promising research directions. In [4], Zhu *et al.* provided a comprehensive review on deep learning in remote sensing, which is focused on automatic target recognition (ATR) and terrain surface classification based on synthetic aperture

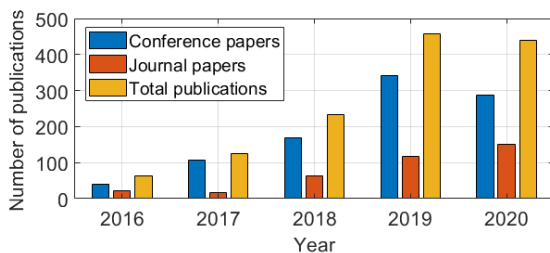


FIGURE 1. Publications on “deep learning for radar” (2016–2020, IEEE Xplore database).

radar (SAR) images. In [5], Zhang *et al.* presented a technical tutorial on the advances in deep learning for remote sensing and geosciences, which is also focused on image classification.

In this work, we conduct a comprehensive review on the application of DL-based algorithms in radar signal processing, which includes the following aspects:

- a) DL for waveform and array design, which is an enabling technology for cognitive radar & spectrum sharing;

The associate editor coordinating the review of this manuscript and approving it for publication was Larbi Boubchir^{ID}.

- b) DL-based radar waveform recognition, which could potentially 1) boost the possibility of intercepting and recognizing the signals transmitted from the low probability of interception (LPI) radar; and 2) improve the direct-path signal estimation accuracy for passive radar applications;
- c) DL-based ATR based on high range resolution profiles (HRRP) profiles, Doppler signatures, SAR images, and other characteristics (e.g. RCS); two limiting factors of the real-life performance of DNNs are emphasized: limited training samples and adversarial examples (note that these two factors are also applicable to DNNs in other application areas in addition to ATR);
- d) DL-based algorithms for jamming/clutter identification and suppression.

The major contributions of this work are summarized as following:

- A comprehensive review of various DL-based algorithms for radar signal processing is provided. The papers reviewed in this work are “hand-picked” high-quality research works and are neatly grouped based on the pre-processing methods, DNN structure, main features, dataset, etc.
- Both the positive and the negative sides of stories about DL are checked. In contrast, in many existing reviews/surveys on this topic, DL has been unanimously praised as a “marvelous” tool that can overcome all the barriers that preventing radar systems reaching the ideal performance goal. In this work, considerable pages are spent on the “negative” side, e.g. the devastating effects of carefully-crafted adversarial examples on an otherwise “well-trained” DL network.
- The relationship between the algorithms proposed in various papers is thoroughly investigated. Generally, a “novel” algorithm doesn’t always pop out from nowhere. By analyzing the evolution process from one algorithm to another by comparing different research works rather than taking the contribution claims made in each paper based on their face values, one can get much deeper insights into the problem at hand and the real contribution of a paper. Specifically, in the field of DL, open-source Matlab/Python codes are free for downloads on many websites. The true value of a specific research paper can only be determined by linking everything together as a full picture and then make observations regarding the position of this particular paper within the whole picture.

The general structure of this review paper is plotted in **Fig. 2**. The techniques/applications investigated in this work are listed in **Fig. 3**, with the most popular network architecture and application highlighted. The rest of this work is organized as following. In Section II, a couple of DL-based radar waveform & array design algorithms are reviewed. In Section III, we focus on the radar signal recognition problem for LPI

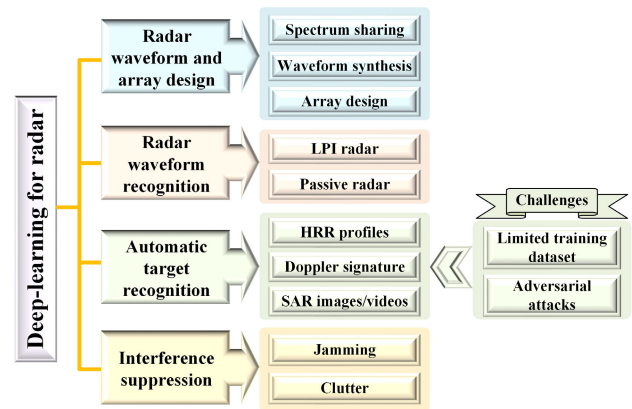


FIGURE 2. Structure of this review.

radar and passive radar. In Section IV, automatic target recognition based on radar HRRP, micro-Doppler signature, and SAR images with DL-based algorithms is investigated. Moreover, two challenging problems for DL-based radar signal processing, namely the lack of training data and the adversarial attacks, are also analyzed. In Section V, various DL-based jamming and clutter suppression algorithms are compared and analyzed. Some final remarks are offered in Section VI.

II. DEEP LEARNING FOR RADAR WAVEFORM AND ARRAY DESIGN

A. DL FOR SPECTRUM-SHARING

With the ever-increasing demand for spectrum resource from wireless communications systems, technologies enabling spectrum-sharing between radar and communications systems have grabbed the attention of researchers from both fields. In [7]–[11], the DL-based algorithms have been employed to prevent mutual interference between radar and communications systems that share the same frequency band. In [7], Smith *et al.* proposed a novel DNN structure made of the *actor network*, which performs actions based on the current environment state, and the *critic network*, which is responsible for judging if the actor’s behavior is appropriate. *Deep deterministic policy gradient* (DDPG)-based reinforcement learning strategy is adopted, and waveforms containing power spectrum notches are designed to constrain interferences from radar to communications systems. In [8]–[9], Thornton *et al.* proposed a novel Double Deep Recurrent Q-Network, which combines the double Q-learning algorithm and the long-short term memory (LSTM), so that radar learns to avoid sub-bands containing interference signals in a spectrum co-existence scenario. DL-based algorithms are also increasingly adopted to solve the problem of target-tracking in congested-spectrum environments. Specifically, researchers from the U.S. Army Combat Capabilities Development Command (DEVCOM) developed a DL-based strategy for radars to autonomously learn the behavior of interferences from co-existing communication systems so that clean spectrum is identified & radar waveforms are

Application codes		Applications							Technique codes		
		ATR			INTERF		WD	WR			
		HRRP	Micro-D	SAR	CLUT	JAM					
Techniques	CNN	4	7	18	8	7	2	9	55	• CNN: Convolutional neural network	
	DBN	2	2	0	0	0	0	0	4	• DBN: Deep belief network	
	DRES	1	0	0	0	0	2	2	5	• DRL: Deep reinforcement learning	
	DRL	0	0	0	0	3	0	2	5	• DRES: Deep residual neural network	
	FNN	1	0	0	0	1	2	0	4	• FNN: Feed-forward neural network	
	GAN	1	0	4	0	0	0	0	5	• GAN: Generative adversarial network	
	RNN	4	0	2	1	3	2	0	12	• RNN: Recurrent neural network, include long-short term memory	
	SAE	1	0	2	0	1	0	0	4	• SAE: Stacked auto-encoder	
	OTHER	2	1	3	1	1	1	1	10	• OTHER: Other neural network	
	Total	16	10	29	9	13	9	14	104		

FIGURE 3. Techniques/Applications investigated in “deep learning for radar” (2016–2020).

modified accordingly [10]. In [11], Kozy *et al.* models the problem of radar tracking in the presence of interference as a Markov Decision Process, and applies deep-Q learning to balance the signal-to-interference-plus-noise ratio (SINR) and the bandwidth usage so that the mutual interferences between radar and the co-existing communications systems is minimized.

B. DL FOR OPTIMIZED WAVEFORM SYNTHESIS

DL-based algorithms are also increasingly adopted in the fields of radar waveform optimization under specific constraints, especially for MIMO radar. In order to separate the echo signals caused by the illuminating signals from different transmitting facilities of MIMO radar for further processing at the receiving end and achieve the waveform diversity gain, the waveforms from different transmitting antennas have to be near-orthogonal [12]. Hence the cross-correlations between waveforms from different transmitting antennas are to be minimized. To minimize the auto-/cross-correlation sidelobes while meeting the constraints of constant modulus, Hu *et al.* designed a deep residual neural network consists of 10 residual blocks, each of which is made of dual layers of 128 neurons [13]. Later, a deep residual network similar to the one in [13] was adopted in [14] to synthesize desired beampatterns while minimizing the cross-correlation sidelobes under the constraints of constant modulus. In [15], Zhong *et al.* proposed a feed-forward neural network with ten hidden layers to maximize the SINR of MIMO radar under the constraints of constant modulus and low sidelobe levels. many research works are focused on the problem of the minimization of cross-correlation sidelobe levels. In [16], the problem of multi-target detection was considered assuming unknown target positions, where deep reinforcement learning based strategy was adopted for waveform synthesis to maximize the detection capabilities of MIMO radar. Finally, the waveform generation and selection problem for multi-mission airborne weather radar was discussed in [17], where a feedforward neural network with varying number of hidden layers was designed to synthesize nonlinear frequency modulated waveforms (NFMW) with pre-determined bandwidth and pulse length.

C. DL FOR ARRAY DESIGN

DL-based algorithms have also been employed to realize cognitive selection and intelligent partition of antenna subarrays. For example, in [18], a CNN with multiple convolutional layers, pooling layers and fully connected layers (referred to as “Conv”, “POOL”, and “FC”, respectively, for simplicity in the rest of this work) was utilized for cognitive transmit/receive subarray selection based on the development of the surrounding environment. Moreover, DL-based algorithms could potentially boost the performance of subarray-based MIMO (Sub-MIMO) radar, which could be regarded as a hybrid of phased-array radar and MIMO radar. The essence of Sub-MIMO radar is to transmit correlated waveforms within the same subarray, which resembles the working mechanism of the conventional phased-array, while the waveforms from different subarrays designed to be orthogonal, so that they could be separated at the receiving end for waveform diversity gain [19]. It follows naturally that the partition of subarrays for Sub-MIMO radar plays a key role in deciding the balance between the coherent processing gain and the waveform diversity gain. In [20], a novel CNN was proposed for interleaved sparse array design for phased-MIMO radar. Specifically, the parallel lightweight structure (i.e. PL module), which is based on the MobileNet-V2 structure, was used to divide feature matrices into parallel branches. Meanwhile, the scale reduced convolution structure (i.e. SR-module) was used as an alternative to the conventional pooling layer for feature matrix dimension reduction. Simulation results show that compared with uniform antenna array partition, the proposed CNN provides transmit beampatterns with narrower mainlobe and lower sidelobes, more accurate direction of arrival (DOA) estimation, and higher output SINR.

The structures of the DNNs proposed in [7]–[20] and their distinctive features are summarized in TABLE 1.

III. DL FOR LPI OR PASSIVE RADAR WAVEFORM RECOGNITION

The DL-based radar waveform recognition is also gaining popularity in recent years. Various neural networks and algorithms have been developed, which include the deep convolutional neural networks (CNNs) [21]–[23], auto-encoders

TABLE 1. DL-based radar waveform and array design.

Reference	DNN structure	Main features	Application
Smith et al. [7]	Actor network (select actions based on environment state) + critic network (evaluate the actor's performance)	<input type="checkbox"/> Deep deterministic policy gradient reinforcement learning <input type="checkbox"/> Design waveforms containing power spectrum notches	Spectrum sharing
Thornton et al. [8]-[9]	Double Deep Recurrent Q-Network (i.e. double Q-learning + LSTM)	<input type="checkbox"/> Radar learns to avoid sub-bands containing interference signals in a spectrum sharing scenario	
Kozy et al. [11]	Deep reinforcement learning	<input type="checkbox"/> Cognitive radar learns and predicts the mutual interference between coexisting radar-communication systems while perform tracking task	
Hu et al. [13]	Deep residual neural network (10 residual blocks, each consists of 2 layers of 128 neurons)	<input type="checkbox"/> Generate waveform of any length for MIMO radar to satisfy the constraints of constant modulus and low auto- & cross-correlation sidelobes	Waveform synthesis
Zhang et al. [14]	Deep residual neural network (5 residual blocks, each consists of 2 layers of 128 neurons)	<input type="checkbox"/> Approximate a beampattern while minimizing cross-correlation sidelobe levels and satisfying the constraint of constant modulus	
Zhong et al. [15]	Feed-forward neural network with ten hidden layers	<input type="checkbox"/> MIMO radar waveform design to maximize the SINR under the constraints of constant modulus and low sidelobe levels	
Wang et al. [16]	Deep reinforcement learning	<input type="checkbox"/> Synthesize waveforms to maximize the detection capabilities of MIMO radar assuming that the number of targets and their positions are unknown	Array design
Kurdzo et al. [17]	Feed-forward neural network with the number of hidden layers varying between 1 and 15	<input type="checkbox"/> Synthesize nonlinear frequency modulated waveforms with specified bandwidth and pulse length	
Elbir et al. [18]	CNN (input layer + 3 × Conv + 2 × POOL + 2 × FC + output layer)	<input type="checkbox"/> Cognitive transmit/receive subarray selection based on the environment	
Cheng et al. [20]	CNN (input + 3 × Conv + 3 SR-modules + 4 PL modules + 1 × POOL + 1 × FC + output)	<input type="checkbox"/> Antenna array partitioning with CNN <input type="checkbox"/> Use PL-modules to divide feature matrices into parallel branches <input type="checkbox"/> Use SR-modules instead of pooling to reduce feature matrix dimension	Array design

[24]–[26], and recurrent neural networks (RNNs) [27]–[29]. These techniques could potentially 1) boost the possibility of intercepting and recognizing the signals transmitted from the low probability of interception (LPI) radar [30]–[31]; and 2) improve the direct-path signal estimation accuracy for passive radar applications [43]–[45]. However, as is pointed out in [46], [47], DL-based signal classification algorithms are vulnerable to adversarial attacks, which are expected to be more powerful than classical jamming attacks.

A. DL FOR LPI RADAR

Most modern radar systems have been designed to emit LPI waveforms to avoid interception and detection by enemies. Therefore, automatic radar LPI waveform recognition has become a key counter-countermeasures technology. In literatures, dozens of DL-based waveform recognition techniques have been proposed within the past five years. Usually, the raw radar data are first pre-processed with time-frequency analysis (TFA) techniques, such as Choi-William distribution (CWD) [30]–[35], Fourier-based Synchrosqueezing transform (FSST) [36], Wigner Ville distribution (WVD) [37], and short-time Fourier transform (STFT) [38]–[40], to obtain the time-frequency images. After that, various DNN structures, mostly CNN, could be designed for feature extraction and waveform classification.

In [30]–[35], the TFA technique (CWD) was used to generate time-frequency images in the pre-processing step. In [30], the sample averaging technique (SAT) was adopted for signal pre-processing to reduce the computational cost, after which a 9-layer CNN was proposed. In [31], a 7-layer CNN along with a novel tree structure-based process optimization tool (TPOT) classifier was designed. In [32], Ma *et al.* employed two different DNN structures to approach the waveform classification problem: a 11-layer CNN and a bidirectional LSTM, with the former exhibiting better performance. In [33], transfer learning was employed to counter the problem of limited training data. The network was pretrained

with five different existing high-performance CNN architectures: VGG16, ResNet50, Inception-ResNetV2, DenseNet, and MobileNetV2, with VGG-16 proved to offer the highest classification accuracy.

Twelve different types of radar waveforms have been used to test the performance of various CNN structures proposed in [30]–[33], which include the linear frequency modulated (LFM) waveform, the BPSK, the Frank-coded waveform, the Costas-coded waveform, the P1-P4 phase-coded waveforms, and the T1-T4 time-coded waveforms. Although the performances of different DNNs in [30]–[33] are noncomparable due to training/test data difference, the classification accuracy offered by these DNNs for SNR = -4 dB are all higher than 90%. In [34]–[35], the performances of DNNs were tested with less than 8 different types of waveforms. In [34], networks (Inception-v3 and ResNet-152) pretrained with ImageNet were used to reduce the training cost. In [35], instantaneous autocorrelation function (IAF) was used for denoising via atomic norm as a pre-processing step, following which a CNN structure was proposed for the classification of the LFM, the Costas-coded, and the P2-P4 coded waveforms.

Although the CWD is a widely adopted TFA technique, it also involves high computational complexity, which makes the researchers to seek computationally-effective alternatives. The FSST was used in [36] as a substitute for CWD in the pre-preprocessing step, following which a multi-resolution CNN with three different kernel sizes was proposed. In [37], the WVD was adopted, and a VGG16 variant pretrained with ImageNet was used to reduce the training cost. Moreover, the STFT was adopted in [38]–[40] to obtain the time-frequency diagram of radar data. In [38], Ghadimi *et al.* proposed two CNN structures based the GoogLeNet and AlexNet, respectively, for the classification of LFM, P2-P4, and T1-T4 waveforms. In [39], Wei *et al.* proposed a novel squeeze-and-excitation network for feature extraction in time, frequency, and time-frequency domains, and the recognition results of all the domains are fused subsequently. In [40],

TABLE 2. DL for radar waveform recognition.

Reference	Pre-processing	DNN structure	Recognized radar waveforms
Kong et al. [30]	<input type="checkbox"/> SAT to reduce computational cost <input type="checkbox"/> TFA technique for CWD-TFI	CNN: $2 \times$ Conv, $2 \times$ POOL, $2 \times$ FC	LFM, Costas, BPSK, Frank, P1-P4, T1-T4
Wan et al. [31]	<input type="checkbox"/> TFA technique for CWD-TFI	CNN: $2 \times$ Conv, $2 \times$ POOL, $2 \times$ FC + TPOT classifier	
Ma et al. [32]	<input type="checkbox"/> Short-time autocorrelation combined with TF analysis	CNN (11 layers) + Bidirectional LSTM	
Lay et al. [33]	<input type="checkbox"/> TFA technique for CWD-TFI	Transfer learning (VGG16, ResNet50, InceptionResNet, DenseNet, MobileNet)	
Guo et al. [34]	<input type="checkbox"/> TFA technique for CWD-TFI <input type="checkbox"/> Pretrained network with ImageNet	Transfer learning (Inception-v3 & ResNet-152)	LFM, Costas, BPSK, Frank, T1-T4
Zhang et al. [35]	<input type="checkbox"/> IAF denoising via atomic norm <input type="checkbox"/> CWD for denoising <input type="checkbox"/> Sparse TF reconstruction	CNN: $3 \times$ Conv, $3 \times$ POOL, $2 \times$ FC	P2-P4, LFM, Costas
Ni et al. [36]	<input type="checkbox"/> TFA with FSST	multi-resolution CNN (3 kernel sizes), feature fusion, classification fusion	LFM, Costas, BPSK, Frank, P1-P4, T1-T4
Pan et al. [37]	<input type="checkbox"/> TFA technique (pseudo WVD) <input type="checkbox"/> Pretrained network with ImageNet (VGG16 variant)	Adaptive layer ($3 \times$ Conv + batch norm) + 2D score layer+1D output	LFM, Costas, BPSK, Frank,
Ghadimi et al. [38]	<input type="checkbox"/> Short Time Fourier Transform (STFT)	CNN (Improved GoogLeNet & AlexNet)	LFM, P1-P4, T1-T4
Wei et al. [39]		“squeeze (global information embedding layers)-and-excitation ($2 \times$ FC)”	BASK, BFSK, BPSK, SW, LFM, NLFM (sin), NLFM (exp)
Orduyilmaz et al. [40]		CNN: $3 \times$ Conv, $1 \times$ FC	20 classes, FM (sawtooth up/downchirp, sinusoidal, stepped up/down chirp, etc.), PM (Barker, Frank, P1-P4, T1-T4)
Yildirim et al. [41]	N/A	Adaptive 1D CNN (4 hidden layers & 2 dense layers)	CW (sinusoid, LFM-up, LFM-up/down, bi-phase coded), pulsed (sinusoid, LFM-up, bi-phase coded, frequency-stepped)

a simple CNN with three convolution layers and one fully connected layer was used to classify of 20 different types of signals, which include frequency-modulated waveforms with various bandwidth and pulse width and phase-modulated waveforms.

Finally, it is worth mentioning that some research works on this topic didn't employ TFA techniques for signal pre-processing. For example, in [41], an adaptive 1D CNN with four hidden layers and two dense layers was proposed for the classification of continuous and pulsed waveforms (sinusoidal, LFM, bi-phase coded, frequency-stepped).

The preprocessing procedures, the DNN structures, and the radar waveforms used for performance evaluation in [30]–[40] are summarized in TABLE 2.

B. DL FOR PASSIVE RADAR

Another potential application area for the DL-based automatic waveform recognition algorithms is passive radar. Passive radar utilizes the signals from illuminators of opportunities (IOs) (e.g. base stations of wireless communications systems) for target detection, imaging, and tracking, which could increase the radar coverage area while avoiding the high infrastructure cost and the spectrum-crowdedness caused by the construction of new dedicated radar transmitters. However, since the waveforms from the IOs are usually unknown to radar receivers, the performance of passive radar is usually much worse than the conventional active radar [42]. In [43]–[44], DL was used to realize simultaneous waveform estimation and image reconstruction for passive SAR composed of a ground-based IO at known position and an airborne receiver. A recurrent neural network (RNN) was designed, with which the scene reflectivity was recovered via forward

propagation, while the waveform coefficients were reconstructed via backpropagation. Simulation results show that the proposed RNN could learn the characteristics of quadrature phase-shifted keying (QPSK) signals [43] and OFDM signals transmitted from DVB-T [44], and perform the SAR image reconstruction with low error. It was also shown that as the number of layers of the RNN increases, the image contrast improves at the cost of increased reconstruction error. In [45], Wang *et al.* developed a novel DNN consisting of a two-channel CNN and bi-directional LSTM, which is termed as TCNN-BL, for waveform recognition for cognitive passive radar, which could modify the sampling rate adaptively to suit the task at hand. Moreover, a parameter transfer approach was utilized to improve the network training efficiency.

C. CHALLENGES

According to [46], the DNNs are highly vulnerable to adversarial attacks. Depending on the information that is available to the attackers, adversarial attacks could be classified as *white-box attack* (the model structure and the parameters of the network are completely known *a priori*), *grey-box attack* (known model structure & unknown parameters), and *black-box attack* (unknown model structure & parameters). In most cases, the detailed information regarding DNNs is unknown to the attacker, who can only get access to the classification results of the network. Although black-box attack is more common and less devastating than the other two types of attacks, white-box attack is often used in research works to evaluate the worst-case scenario. In [47], Sadeghi *et al.* showed that black-box attack can be designed to be approximately as effective as white-box attack, which could lead to dramatic performance degradation in DL-based radio signal

classification. It is worth noting that most research works on the topic of signal/waveform misclassification caused by adversarial attacks target the wireless communication systems rather than radar. Nevertheless, the theory and mechanism of adversarial attacks for these two closely related fields are identical. To encounter the challenges posed by adversarial examples, various adversarial training and detection approaches have been developed. For example, in [48], the 1D CNN used as RF signal classifier was pre-trained with an autoencoder to mitigate the deceiving effects of adversarial examples, which has the potential to be extended to the 2D image classification problem. In [49], two statistical tests were proposed for the detection of adversarial examples.

IV. DL FOR ATR

Machine learning (such as k-nearest neighbor and dictionary learning) has been employed for ATR long before the emergence of DL [50], [51]. After AlexNet (one of the most popular deep CNNs) won the ILSVRC'12 contest [52], DL for radar ATR has become an intensively researched subject. Based on the amount of labeled data in the dataset used for training the network, DL could be classified as unsupervised learning, supervised learning, and semi-supervised learning (SSL), with SSL being a halfway between the other two. According to [53], in common cases, 1%-10% of the data used for SSL training are labeled, while the rest are unlabeled samples. Since most of the existing DL-based radar ATR methods are supervised, the recognition/classification accuracies of these methods are heavily limited by the amount of labeled training data. In this section, we provide a comprehensive review of DL-based ATR methods proposed in recent published research works, which includes i) ATR using the HRRP; ii) ATR using the micro-Doppler signatures; iii) ATR for SAR; and iv) major challenges for DL-based ATR.

A. DL-BASED ATR USING HRR PROFILES

In order to perform ATR using the HRRP, some pre-processing procedures are often required to eliminate the sensitivities of the DL-based algorithm to time-shift, amplitude-scaling, and aspect-angle. Commonly used sensitivity removal approaches include time-shift compensation, energy normalization, and average processing [54]–[56]. The DNN structures used for radar HRRP target recognition include the deep belief network [54], [55], recurrent attentional network [57], [58], concatenated neural network, CNNs [62]–[64], stacked auto-encoder (SAE) [65], and convolutional LSTM [66], [67].

Some researchers used measured HRRP data for performance evaluation. For example, the HRRP data from Yak-42 (large jet), Cessna Citation S/II (small jet), and An-26 (twin-engine turboprop) were used in [54]–[58]; the HRRP data from Airbus A319, A320, A321, and Boeing B738 were used in [59]; the HRRP data from seven types of ship of different sizes (length from 89.3 m to 182.8 m) were used in [60]; the HRRP data from various types of ground vehicles were used in [62], [66], [67]. Since most researchers only

have access to a limited mount of HRRP measurement data associated with a handful of vehicles, many of them resort to simulated HRRP data generated by software based on the specific CAD models of vehicles for research purposes. For example, in [63], Lundén *et al.* generated HRRP data for 8 fighters (F-35, Eurofighter, etc.) with POFACETS & 3D facet models of aircrafts. In [64], the HRRP data for 6 military and 4 civilian ship targets are simulated based on CAD models assuming X-band maritime radar. Another feasible alternative is data augmentation with generative adversarial network (GAN). Specifically, in [62], GAN was adopted to address the problem of unbalanced training samples, i.e. the labeled training samples for some classes (*majority classes*) significantly outnumber the other classes (*minority classes*).

The DNN structures of the DL-based ATR methods proposed in [54]–[65] along with their distinctive features are summarized in TABLE 3. The preprocessing procedures and the dataset used for performance evaluation have also been noted in the table. It is worth mentioning that some simulation results regarding target recognition using a supervised DL based on the HRRPs collected with MIMO radar have also been presented [68]. However, since the DNN used to obtain the results in [68] was not detailed, it is not included in TABLE 3.

B. DL-BASED ATR USING MICRO-DOPPLER SIGNATURES

DL-based target detection/classification based on micro-Doppler signatures has been gaining ground rapidly in the field of automatic ground moving human/animal/vehicle target recognition [69]–[73] and drone classification [74]–[77]. In [69], MAFAT dataset, which contains the echo signals from humans and animals collected by different pulse-Doppler radars at different locations, terrains, and SNR, was used for the training of a six-layer CNN. To achieve higher classification accuracy, the data was further augmented via random frequency/time shifting, noise-adding, and vertical/horizontal image flipping. In [70], a CNN composed of 5 *dense blocks* (i.e. 3×3 Conv followed by 1×1 Conv) and 5 *transition blocks* (i.e. 1×1 Conv followed by 2×2 POOL) was proposed for human motion classification based on micro-Doppler signatures, the performance of which was tested with two datasets containing the echoes associated with six human motions (walking, running, crawling, forward jumping, creeping, and boxing) obtained via simulation and measurement, respectively. The major feature of the human motion recognition algorithm in [70] is that the proposed network is more robust to the varying target angle aspect than most classic CNN models, such as VGGNet, ResNet, and DenseNet. In [71]–[73], Hadhrami *et al.* investigated the problem of single-person/group/vehicle recognition based on micro-Doppler signatures with DL. Pre-trained classic CNN models (such as VGG16, VGG19, and AlexNet) and transfer learning were adopted to improve the network training efficiency. The RadEch human/vehicle targets tracking data collected with Ku-band pulse-Doppler radar, which covered typical scenarios like single-person/group walking/running

TABLE 3. Radar HRRP target recognition with deep networks.

Ref.	Preprocessing	DNN structure	Main features	Dataset	Public-domain available?
Feng et al. [54]	Time-shift compensation, energy normalization & average processing for sensitivity elimination	□ Deep belief network (one Gaussian–Bernoulli RBM layer + two conventional RBM layers) □ Stacked denoising autoencoder	□ Incorporate HRRP frame & average processing into one autoencoder □ Robust to noisy observation	HRRP data from Yak-42 (large jet), Cessna Citation S/II (small jet), and An-26 (twin-engine turboprop)	Yes
Pan et al. [55]		Deep belief network (stacked RBMs) + softmax	□ Use t-SNE to deal with imbalanced distribution among different targets & aspects		
Zhao et al. [56]	Energy normalization to eliminate amplitude-scaling sensitivity	Semi-supervised multitask recognition: deep-u-blind denoising network (autoencoder - decoder) + recognition phase (AlexNet variant)	□ Feature maps of encoder are transferred to decoder through the fusion layers to avoid gradient vanishing	HRRP data from civilian aircrafts (Airbus A319, A320, A321, Boeing B738)	Yes
Xu et al. [57][58]	Dividing HRRP data into multiple overlapping sequential features	Target-aware recurrent attentional network (input + encoder layer + attention mechanism)	□ Robust to time-shift sensitivity due to memory & attention mechanism		
Liao et al. [59]	Time-shift compensation, energy normalization, embedding secondary-label (i.e. target aspect angle) in the model	Concatenated neural network consisting of 3 independent shallow neural sub-networks	□ Samples of target are divided into 4 sub-classes based on aspect angle to reduce target-aspect sensitivity □ Recognition results of multiple samples are fused	HRRP data from civilian aircrafts (Airbus A319, A320, A321, Boeing B738)	No
Guo et al. [60]	Energy normalization & average processing for sensitivity elimination	Deep 1D residual-inception network (Conv + POOL + residual-inception block + inception-POOL + FC)	□ Multi-scale conv kernels to extract features with different precisions and possess weight-sharing property □ Novel loss function considering inter-class/intra-class distance	Seven types of ship of different sizes (length from 89.3 m to 182.8 m)	No
Song et al. [61]	Energy normalization, training data augmentation with shifting (translation)	Multi-channel CNN (3 × Conv + 3 × POOL + 2 × FC)	□ Multi-channel input (real-imaginary, amplitude-spectrum) □ Use “deep features” generated by the final conv layer instead of handcrafted features	Four classes of unspecified ground targets with different HRRP	No
Song et al. [62]	Target section segmentation, padding & normalization for noise & clutter elimination in GAN training	Deep convolutional generative adversarial network consisting of generator & discriminator made of 1D convolutional operators	□ GAN for HRRP generation □ Unbalanced training samples (i.e. majority vs minority class) □ 2 novel 1D convolutional operators, SC & FSC, are used	6 classes of vehicles (Sedan, Jeep, MPV, tractor, farm vehicle, box truck)	No
Lundén et al. [63]	Energy normalization to eliminate amplitude-scaling sensitivity	CNN (2 × Conv + 2 × POOL + 3 × FC)	□ Multistatic radar system □ The HRRPs of targets are calculated with POFACETS & 3D facet models of aircrafts	8 fighters (F-16, F-35, F-18, MQ-1, PAK FA T-50, JAS-39C, Eurofighter, Rafale)	No
Karabayır et al. [64]		CNN (4 × Conv + 2 × POOL + 1 × FC)	□ HRRPs are simulated based on target CAD models and then converted to 2D images □ Simulation infrastructure from MatConvNet is used	HRRPs simulated based on CAD models of 6 military & 4 civilian ship targets assuming X-band maritime radar	No
Liu et al. [65]		Frame maximum likelihood profile (FMLP)-trajectory similarity auto-encoder (stacked autoencoders)	□ FMLP is used to characterize all HRRP signals in a specific frame rather than centroid alignment used in [54]	Three aircraft targets (D507, D715, D910)	No
Zhang et al. [66][67]	Data alignment & normalization to reduce time-shift & amplitude sensitivity; data reshaping with coding module (raw fully polarimetric data coded into real matrix)	Self-attention module (focus on specific range cells) + 2 × Conv LSTM layers with 1 × POOL between them + classification module (FC + softmax)	□ Polarimetric HRRP recognition □ Collect scattering information from both spatial and 4 polarimetric dimensions □ Focus on discriminative range cells for learning capacity improvement	10 vehicles (Camry, Civic, Jeep93, Jeep99, Maxima, Mazda MPV, Mitsubishi, Sentra, Avalon, Tacoma) [66]; 4 vehicles (truck, pick-up, sedan, minibus) [67]	Yes

and truck moving, was used to test the performance of the proposed network. Moreover, data augmentation ($\times 16$) with image vertical flipping and circular shifting was employed to compensate for the limited training data.

In [74] and [75], pretrained classic CNN models (e.g. GoogLeNet) are used for drone classification. Specifically, in [74], the micro-Doppler signatures and the

cadence-velocity diagrams obtained by 14 GHz frequency modulated continuous wave (FMCW) radar in indoor/outdoor experiments are merged as Doppler images, based on which drones with different number of motors are classified. In [75], both the pretrained GoogLeNet and the deep series CNN with 34 layers are employed for in-flight drone/bird classification. The RGB and the grayscale echo

signal dataset collected by 24 GHz and 94 GHz FMCW radars are used to train the two networks, respectively. One distinctive feature of the networks presented in [75] is that clutter and noises have been treated as two separate subclasses. In [76] and [77], Mendis *et al.* proposed a deep belief network (DBN) formed by stacking the conventional RBM and the Gaussian Bernoulli RBM (GBRBM), which is similar to the one proposed in [54], to address the problem of micro drone detection and classification. The classification was based on the Doppler signatures of the targets of interest and their spectral correlation function (SCF) (i.e. Fourier transform of autocorrelation function) signature patterns. The performance of the proposed DBN was tested with the echo signals collected from three micro-drones (available at supermarkets at a price lower than \$100) by S-band CW Doppler radar. The micro-Doppler signature based target detection and classification approaches proposed in [69]–[77] are summarized in TABLE 4.

Finally, it is worth mentioning that a comprehensive review on the application of DL for UAV detection and classification was provided in [78]. Although [78] covers the general topic of drone detection with multi-types of sensors (which include electro-optical, thermal, sonar, radar, and radio frequency sensors) and does not focus specifically on drone classification using the Doppler signatures collected by radar, it still serves as a good reference work for readers who are interested in the topic of drone/birds detection and classification.

C. DL-BASED ATR FOR SAR AND VIDEO SAR

In 2020, Majumder, Blasch, and Garren published a book summarizing recently proposed DL-based approaches for radar ATR, where DL for single and multi-target classification in SAR imagery was considered [79]. Specifically, this book focused on the ATR performances of various DNNs evaluated with the popular *MSTAR* dataset, with *MSTAR* stands for the Moving and Stationary Target Acquisition and Recognition. The public release of the *MSTAR* dataset, which was collected by the Defense Advanced Research Projects Agency (DARPA) and the Air Force Research Laboratory (AFRL), consists of 20,000 SAR image chips covering 10 targets types from the former Soviet Union. It should be noted that, although the *MSTAR* dataset has long been widely adopted in research works to evaluate the performance of traditional machine-learning based algorithms (e.g. SVM), by which a classification rate of 97%–100% had been reached, it has been shown in some papers that the ATR performance of the algorithms trained/tested merely on the *MSTAR* dataset usually degrade when trained/tested using other dataset (e.g. the QinetiQ dataset [80], [81]). Nevertheless, in this section, we will give a brief review of recently proposed DNNs for ATR employing the *MSTAR* dataset [82]–[92] and other SAR image datasets (e.g., TerraSAR-X). The limitation of the *MSTAR* dataset and the possible counter solutions will be covered later in Section IV-D.

In [82], Chen *et al.* proposed an all-convolutional network (A-ConvNet) composed of 5 Conv and 3 × POOL.

Since only sparse connected Conv were used and the FC was omitted, A-ConvNet is highly computational efficient. The performance of A-ConvNet was evaluated under both standard operating condition (SOC) and extended operating condition (EOC) (e.g. substantial variation in depression angle/target articulation), which has been widely adopted as the performance benchmark in research papers. In [83], a normal multiview deep CNN (DCNN) was proposed, which is a parallel network with multiple inputs (i.e. SAR images from different views) requiring only a limited amount of raw SAR images. The features learned from different views are fused progressively toward the last layer of the network, which leads to classification rates of 98% and 93% for SOC and EOC, respectively. In [84], Furukawa *et al.* proposed a CNN termed as verification support network (VersNet) composed of an encoder and a decoder. A main feature of the network is that the input SAR image could be of arbitrary size and consisting of multiple targets from different classes. In [85], Shang *et al.* added an information recorder, which is a variant of the *memory module* proposed in [89], along with a mapping matrix to the basic CNN. The resulting memory CNN (M-Net) uses spatial similarity information of recorded features to predict unknown sample labels. A two-step training process (i.e. parameter transfer) was employed to guarantee convergence of the results and to reduce the required of training time. The CNNs proposed in [86]–[88] are also worth brief mentioning. In [86], morphological operation was used to smooth edge, remove blurred pixel, amend cracks, and the large-margin softmax batch normalization was employed. In [87] and [88], the database was extended with affine transformation in range, and a couple of SVMs were used to replace the FC in CNN for final classification.

ATR based on SAR image sequence obtained from, for example, single-radar observations along a circular orbit over time or joint observation from different angles by multiple airborne radars, has also been investigated in research works. Considering that the sub-images in the SAR image sequence obtained by the imaging radar over a period of time from the same target often exhibit conspicuous variations, a spatial-temporal ensemble convolutional network (STEC-Net) consisting of 4 convolutional layers and 4 pooling layers was proposed in [90]. Dilated 3D convolution was used to extract spatial and temporal features simultaneously, which were progressively fused and represented as the ensemble feature tensors. To reduce the training time, compact connection was used rather than fully connected layer. In [91], Zhang *et al.* proposed a multi-aspect-aware bidirectional LSTM network (MA-BLSTM) consisting of the feature extraction blocks, the feature dimension reduction block, and 3-layer LSTM block. The feature extraction block utilizes the Gabor filter (orientation and rotation sensitive) in combination with the three-patch local binary pattern (TPLBP) operator (rotation invariant) to obtain global & local features, while 3-layer MLP was employed for feature dimension reduction. In [92], Bai *et al.* proposed a bidirectional LSTM network, the performance of which was evaluated for two cases: clutter-present

TABLE 4. DL-based target detection & classification using micro-Doppler signatures.

Reference	Preprocessing	DNN structure	Main features	Dataset	Public-domain available?
Dadon et al. [69]	STFT + FFT shift + abs(.) + log(.) + norm(.)	CNN (2 × Conv + 2 × POOL + 2 × FC)	<input type="checkbox"/> Data augmentation with random frequency/time shifts, noising, flipping	MAFAT dataset (echo signals from humans & animals within coverage area of pulse-Doppler radar)	Yes
Yang et al. [70]	STFT + average background subtraction	CNN (5 dense blocks + 5 transition blocks + output); <u>dense block</u> : 2 × Conv; <u>transition block</u> : 1 × Conv + 1 × POOL	<input type="checkbox"/> Insensitive to angle aspect (i.e. the target moves in arbitrary direction)	Simulation & measurement dataset: 6 human motions (walking, running, crawling, forward jumping, creeping, boxing)	No
Hadhrami et al. [71][72][73]	Short-time Fourier Transform (STFT)	Pretrained CNN (VGG16 & VGG 19 [71][73]; AlexNet [72][73])	<input type="checkbox"/> Pre-trained CNN model & transfer learning <input type="checkbox"/> Data augmentation (16 x) with vertical flipping & circular shifting	RadEch tracking data collected with Ku-band pulse-Doppler radar (one-person walking/running/crawling; group walking/running, wheeled, truck, clutter)	Yes
Kim et al. [74]		CNN - pretrained model (GoogLeNet)	<input type="checkbox"/> Micro-Doppler signature & cadence-velocity diagram are merged as Doppler image	Micro-Doppler signatures of drones with different number of motors measured by 14 GHz FMCW radar in indoor/outdoor experiments	No
Rahman et al. [75]		2 networks: pretrained CNN (GoogLeNet) & deep series network (CNN with 34 layers)	<input type="checkbox"/> RGB & grayscale dataset are used for training GoogLeNet & the proposed series network, respectively <input type="checkbox"/> Clutter & noise are regarded as sub-classes	Echo signals from inflight drones and birds collected by 24 GHz & 94 GHz FMCW radar	No
Mendis et al. [76][77]	Cyclic autocorrelation function + FFT	Deep belief network (Gaussian–Bernoulli RBM + RBM layers, similar to [54])	<input type="checkbox"/> Spectral correlation function (SCF) pattern signature is used <input type="checkbox"/> Resilient to white Gaussian noise	Echo signals collected from three micro unmanned aerial systems by S-band CW Doppler radar	No

and clutter-free. Surprisingly, the presence of clutter lead to higher classification accuracy than the clutter-free case. All the DNNs proposed in [90]–[92] reported a target recognition accuracy higher than 99.9%, but the performance is expected to degrade in real-life application scenarios (note: “a machine trained in one environment cannot be expected to perform well when environmental conditions change”—Pearl [93]).

According to [91] and [92], the LSTM network outperforms the hidden Markov models (HMMs), which has been widely adopted to model the multi-aspect SAR images until 2000s [94], in modeling the stochastic sequences, especially when the initial probability of states is unknown. However, the LSTM is notoriously time-consuming to train (not to mention that the training time of MA-BLSTM increases by *5 times* with the decrease of training data [91]). Moreover, auto-extracted features obtained with CNNs or other types of unsupervised neural networks are not necessarily better than the hand-crafted ones designed by human experts. Actually, many well-established researchers hold doubts against the “black-box” process of “automatic” feature extraction, which makes a network extremely vulnerable to adversarial attacks (more details regarding this problem will be provided in Section IV-D).

Except for the CNNs and the LSTM networks mentioned above, other DL-based networks such as the autoencoders and Capsule Networks (CapsNets) have also been investigated as feasible solutions to the ATR problem. In [95], Deng et al. proposed a network composed of stacked auto-encoders (SAE). To avoid overfitting, restriction based on Euclidean distance was implemented (i.e. samples from the same target at different aspect angles have shorter distance in feature space) and a dropout layer was added to the network.

In [96] and [97], Geng et al. proposed a deep supervised & contractive neural network (DSCNN), which consists of 4 layers of supervised and contractive autoencoders. Multiscale patch-based feature extraction was performed with three filters: the gray-level gradient cooccurrence matrix (GLGCM) filter, the Gabor filter, and the histogram of oriented gradient (HOG) filter. The graph-cut-based spatial regularization was applied to smooth the results. Moreover, unlike the other networks discussed in this subsection, which have all been trained and tested using the MSTAR dataset, the DSCNN was tested with three datasets, the TerraSAR-X, the Radarsat-2, and the ALOS-2 data. A comprehensive review of autoencoder and its variants for target recognition in SAR images could be found in [98]. In [99]–[102], various capsule networks (CapsNets) were proposed to address two problems in SAR-image based ATR: limited training data and depression angle variance. CapsNets are composed of capsules which are vectors of information about the input data, with the magnitude representing the probability of the presence of an entity and the direction representing the pose and position of the entity. Due to page limitation, this minority group of CapsNets based networks won’t be detailed here. The DNNs discussed in this section for ATR using SAR images are summarized in TABLE 5.

Finally, note that DL could also be used for video-SAR moving target indication. Specifically, Ding et al. proposed a faster region-based CNN in [103], which is a variant of the algorithm proposed by Ren et al. in [104]. To reduce the training burden, the features were extracted with pertained CNN models such as AlexNet, VGGNet, and ZFNet. The Density-based Spatial Clustering of Application with Noise (DBSCAN) algorithm was developed to reduce false

TABLE 5. DL-based target classification using SAR images.

Reference	Preprocessing	DNN structure
Chen et al. [82]	N/A	All-convolutional networks (A-ConvNets) without FC layers ($5 \times \text{Conv} + 3 \times \text{POOL}$)
Pei et al. [83]	SAR images are rotated & aligned to the same aspect angle	Multiview DCNN (parallel network with multiple inputs): $4 \times \text{Conv} + 3 \times \text{POOL} + 1 \times \text{FC}$
Furukawa et al. [84]	Labeling images (10 target classes + target front/background class)	VersNet: encoder ($10 \times \text{Conv} + 4 \times \text{POOL}$, VGG variant) + decoder ($1 \times \text{transposed Conv}$)
Shang et al. [85]	N/A	Memory CNN – M-Net: basic CNN ($5 \times \text{Conv} + 3 \times \text{POOL}$) + mapping matrix + information recorder (index + key + value + time, variant of memory module in [89])
Zhou et al. [86]	Morphological operation to smooth edge, remove blurred pixel, amend cracks	Large-margin softmax batch normalization (LM-BN), CNN (A-ConvNet in [82])
Wagner et al. [87][88]	SAR images are rotated & aligned to the same aspect angle	CNN (feature extraction + decision) + SVM (polynomial kernel & Gaussian radial basis functions)
Xue et al. [90]	Multi-aspect space-varying image sequence construction	Spatial-temporal ensemble convolutional network (STEC-Net): $4 \times \text{Conv} + 4 \times \text{POOL}$
Zhang et al. [91]		Multi-aspect-aware bidirectional LSTM network (MA-BLSTM): feature extraction + 3-layer MLP + 3-layer LSTM block
Bai et al. [92]	N/A	Bidirectional LSTM network (BCRN): $4 \times \text{Conv} + 3 \times \text{POOL} + 2 \text{ Bi-LSTM layers}$
Deng et al. [95]		SAE with Euclidean distance constraint & dropout + linear SVM classifier
Geng et al. [96][97]	Multiscale patch-based feature extraction	Deep supervised & contrastive neural network (DSCNN): 4 layers of supervised & contrastive autoencoders
Guo et al. [99]; Schwegmann et al. [100], [101]; Shah [102]	N/A	Capsule network

alarms, and the Bi-LSTM was used to improve the detection probability. The performance of the proposed network was evaluated with both simulated video SAR data and real data released by Sandia National Laboratory, which was further augmented with rotation and cropping.

D. MAJOR CHALLENGES FOR DL-BASED ATR

In Section IV-C, we reviewed many DNNs trained and tested with the MSTAR dataset. In this subsection, we will look into two limiting factors which have been keeping the unanimous adoption of DNNs for radar ATR tasks on battle fields from becoming true: the limited amount of training data and the potential security risk posted by carefully crafted adversarial attacks.

1) LACK OF TRAINING DATA

Although classification rates of higher than 99% have been reported in many papers covering DNNs trained for radar ATR using the MSTAR dataset, the accuracies of these networks are expected to degrade dramatically when tested with SAR images taken at depression angles that are very different from the ones used to obtain the training dataset or other SAR image datasets, e.g. the QinetiQ dataset [80], [81]. As pointed out by J. Pearl, the neural networks usually cannot perform well if the environment they are tested in is different from the one they are trained with [93]. However, the DL-based approaches will simply lose all their glamor if we must train the network from the very beginning with large amount of qualified training data for every new classification task. What's worse, unlike other ordinary image classification tasks (e.g. cat/dog classification), the SAR images used for radar ATR are usually very scarce, especially when the targets are military vehicles employed by other countries. Therefore, machine learning with small training data sets is key to the success of radar ATR using SAR images. In the following, we will examine various neural networks that are designed to meet this challenge.

Since these networks have all been trained using the MSTAR dataset, the classification accuracies of these networks and the number of samples involved in the training process are comparable. Before we move on, we will first provide some details on the MSTAR dataset, so the readers could get a clear picture of what is happening. As was mentioned before, the MSTAR dataset consists of 20,000 SAR image chips covering 10 targets types from the former Soviet Union (BMP2, BTR70, T72, BTR60, 2S1, BRDM2, D7, T62, ZIL131, ZSU23/4). These targets were measured over the full 360° azimuth angles and over multiple depression angles (15° , 17° , 30° , and 45°), and the SAR images are 128×128 pixels in size and of 1 foot \times 1 foot resolution. In most of papers, to demonstrate the robustness of the proposed networks to the variation of angles, the SAR images used for training and testing usually correspond to two different depression angles (e.g. 15° and 17°).

a: SUPERVISED LEARNING

For comparison purpose, we first look at the application of traditional machine learning method to address this problem. The topic has been thoroughly reviewed in [105]. More recently, in [106], Clemente et al. utilized *K-nearest neighbor* for ATR against compound Gaussian noise, which was added to the MSTAR datasets manually. The features were represented by Krawtchouk moments, and the selection of testing/training samples were randomized in each Monte Carlo run. Using only 191 training samples, the network proposed in [106] reached an accuracy of 93.86%.

b: SEMI-SUPERVISED LEARNING

Since the manual feature extraction usually induces high computational complexity while the auto feature extraction is a time-consuming process requiring a large amount of labeled training samples, some researchers resort to semi-supervised machine learning. In [107], Hou et al. introduced a

semi-supervised online dictionary learning algorithm, where the SAR images were modeled with complex Gaussian distribution (CGD). The dictionary was updated by adding samples to the training process in a progressive way, and the Bayesian inference was employed to learn the dictionary. In [108], Wang *et al.* used dual-networks and cross-training (i.e. the Siamese network) to improve the classification rate with limited training data. Specifically, the pseudo-labels generated by one network were used to fine-tune the other network, and an iterative categorical cross-entropy function was designed as the loss function of the dual-networks for contrastive learning. Although a high accuracy of 97.86% was obtained in [108] with only 400 training samples, it is worth noting that the Siamese network is famous for its sensitivity to input variations and weak generalizability. *Feature augmentation*, i.e. combining complementary features extracted by optimally-selected multi-level layers rather than utilizing the high-level features only, is another solution to improve the accuracy with limited training samples. In [109], Zhang *et al.* proposed a CNN composed of 5 Conv layers, 5 pooling layers, and 2 FC layers. The features from the Conv layers were concatenated, and the AdaBoost rotation forest (RoF) was used to replace the original softmax layers. With 500 training samples, the networks proposed in [109] reach a classification rate 96.3%. Note that other supervised classifiers, such as SVM and random forest, could also be used as substitutes for the softmax layers of a classic CNN to improve the accuracy.

c: UNSUPERVISED LEARNING

One way to realize unsupervised learning with limited training data samples is to employ transfer learning. In [110], Huang *et al.* proposed a DNN composed of stacked convolutional auto-encoders, which was trained with unlabeled SAR images for the subsequent transfer learning rather than the commonly used ImageNet, which contains optical images that are far different from SAR images. In [111]–[118], data augmentation was performed to boost the training dataset in addition to transfer learning to further improve the classification accuracy. Specifically, in [111], Zhong *et al.* employed three classic CNNs, namely CaffeNet, VGG-F, and VGG-M, that have been pretrained with the ImageNet dataset. The data augmentation method used in [82] was adopted, and 2700 images for each class were obtained via randomly sampling 88×88 patches from the 128×128 SAR image chips. With network pruning (a maximum of 80% filters pruned) and recovery employed, the networks presented in [111] is 3.6 times faster than the A-ConvNets proposed in [82] at the cost of 1.42% decrease in accuracy. In [112], Ding *et al.* an all-in-one 6-layer CNN was proposed, and three types of data augmentation, namely posture synthesis, translation, and noise-adding were combined. With training samples augmented to 1000 per class, the network in [112] reached a test accuracy of 93.16%. In [113], Yu *et al.* proposed a 13-layer CNN, with the input data preprocessed with Gabor filters. The center 88×88 pixels of the SAR images were cropped to

reduce the computational burden, and the training dataset was augmented with the approach proposed in [112]. By replacing 1%-15% pixels in target scene with randomly generated samples, the anti-noise performance of the proposed network was demonstrated. In [114], data augmentation was performed by first using improved Lee sigma filtering to remove speckles and then adding random noises. The proposed 9-layer CNN reached a high accuracy of 98.7% with 1900 training samples.

In [115] and [116], Lewis and Scarnati pointed out that the synthetic SAR images obtained by simply manipulating the real SAR images as the ordinary optical images are of poor quality (despite of the resemblance between them in “appearance”), and using only the synthetic data in the training process could lead to dramatic performance degradation. For example, the SAR ATR CNN in [117] achieved only a 19.5% accuracy when trained with synthetic data and tested with real data. Therefore, in [115] and [116], 3D CAD models of targets were used to synthesize the Synthetic and Measured Paired and Labeled Experiment (SAMPLE) dataset. The input data was preprocessed with t-SNE for dimension reduction, and variance-based joint sparsity was employed for denoising. Moreover, the clutter was transferred from real to synthetic SAR images via task masks. With 50% real data from the MSTAR dataset and 50% synthesized data generated with the GAN, the modified DenseNet proposed in [115] reached an accuracy of 92%. In [118], dual parallel GAN (DPGAN) made of a generator with 4 convolution layers and 4 deconvolution layers and a discriminator with 4 convolution layers was proposed. The raw images with opposite azimuth were merged together for shadow compensation. With 300 GAN-augmented training samples, the 5-layer CNN proposed in [118] reached a high accuracy of 99.3%.

The networks proposed in [106]–[118] along with the number of MSTAR samples used for training and the corresponding accuracies are summarized in TABLE 6, where “AUG” represents training data augmentation. Since transfer learning plays a key role in improving the accuracy of DNNs with limited training data while reducing the training time, the readers are also referred to [119], in which how to apply transfer learning in SAR ATR were discussed in detail (note that it was concluded in [119] that simple “domain adaption based transfer learning” by applying a DNN model pretrained with natural optical images, e.g. ImageNet, directly to the problem of SAR image classification/recognition does not work well). Finally, although the MSTAR data set has been widely used for the training of SAR ATR DNNs [106]–[118], some researchers resort to a few SAR image datasets obtained by TerraSAR-X that have been made available to public, which include the landscape mapping dataset [120], the ship detection dataset [121], [122], and the vehicle detection dataset [123].

2) ADVERSARIAL ATTACKS

According to literatures, one most intriguing feature of adversarial attacks is that by slightly changing some pixels of a

TABLE 6. Techniques for machine learning with small training dataset.

Reference	Image size	Neural network	Training samples	Accuracy
Clemente et al. [106]	128 x128	K-nearest neighbor (with Krawtchouk moments used as input)	191	93.86%
Hou et al. [107]	64 x 64	Image modeling with CGD + Bayesian method for learning + dictionary update by adding samples	720	94.52%
Wang et al. [108]	128 x128	Dual-networks & cross-training (Siamese)	400	97.86%
Zhang et al. [109]	128 x128	CNN (5 × Conv + 5 × POOL + 2 × FC + AdaBoost ensemble)	500	96.3%
Huang et al. [110]	128 x128	SAE with 5 × Conv & 1 × FC	500	97.15%
Zhong et al. [111]	88 x 88	Pretrained CaffeNet, VGG-F, VGG-M with ImageNet + transferred network with pruning filters & recovery	2700/class AUG	98.39%
Ding et al. [112]	128 x128	All-in-one CNN (3 × Conv + 2 × POOL + 1 × FC)	1000/class AUG	93.16%
Yu et al. [113]	88 x 88	Preprocessing (multiscale Gabor filter) + CNN (9 × Conv + 4 × POOL)	550, AUG	92%
Kwak et al. [114]	88 x 88	CNN (4 × Conv + 4 × POOL + 1 × FC)	1900, AUG	98.7%
Lewis et al. [115]; Scarnati et al. [116]	128 x128	CNN (DenseNet)	2732 (50% measured +50% synthesized, GAN)	92%
Zhu et al. [118]	128 x128	DPGAN + CNN (4 × Conv + 1 × POOL)	300/class, GAN	99.3%

picture (changes so trivial that humans can't even notice), the DL-based image classification algorithm will be fooled to make unbelievable mistakes. For example, if we add a toaster sticker to a banana, it could be misclassified as toaster by a DL-based classifier [46]. Based on the adversary's knowledge on the network to be attacked, adversarial attacks could be classified as *white-box*, *grey-box* and *black-box attack* (see Section III-C for details). Moreover, an adversarial attack is said to be "targeted" if the adversarial examples have been designed to be misclassified as a specific type of target and "nontargeted" otherwise. The research in the field of adversarial attacks resembles a cat-and-mouse game: many algorithms are designed to misguide the existing DNNs into misclassification, while the others are developed to improve the robustness of the DNNs to adversarial examples via adversarial training, adversarial detection, gradient-masking, etc. In this subsection, we will give a brief introduction to several highly-cited adversarial attack algorithms proposed in recent years. Before we move on to introduce original research works on this topic, we will first provide some background information on commonly used attack methods that are readily available as Python toolboxes free for download [124].

The adversarial attacks widely adopted by DNN attackers generally belong to three categories: the *gradient-based attacks*, the *score-based attacks*, and the *decision-based attacks*.

The gradient-based attacks utilize the input gradients to obtain perturbations that the model predictions for a specific class are most sensitive to. The *fast gradient sign method (FGSM)*, the *Basic Iterative Method (BIM)*, the *iterative least-likely class method (ILCM)*, the *Projected Gradient Descent (PGD)* and the *DeepFool* are some of the most famous attack methods belong to this group [124]. The *FGSM* proposed by Goodfellow et al. [126] utilizes the loss function with respect to the input to create an adversarial example that maximizes the loss so that it will be misclassified. The *BIM*, which is also referred to in literatures as the iterative fast gradient sign attack method (I-FGSM), and the *ILCM* were all proposed by Kurakin et al. in [127]. The *BIM* is a straightforward extension of the *FGSM* method, which seeks to maximize the cost of the true class along small steps in the gradient direction in an iterative manner. In contrast,

the *ILCM* iteratively maximize the probability of specific false target class with lowest confidence score for clean image. The *PGD*-based attack method [128] is essentially the same as the *BIM* except that for *PGD*, the example is initialized at a random point in the ball of interest determined by the ℓ_∞ norm. The *DeepFool* method proposed by Moosavi-Dezfooli [129] first computes the minimum distance it takes to reach the class boundary assuming that the classifier is linear, then makes corresponding steps towards that direction.

The score-based attacks do not require gradients of the model or other internal knowledge about the networks to be attacked, but need to know the probability that the input samples belong to a certain class, i.e. the probability labels. It is less popular than the gradient-based attacks. The *single-pixel attack* proposed by Narodytska and Kasiviswanathan [130] in 2017 is a typical score-based attack. It probes the weakness of a DNN by changing single pixels to white or black one at a time. In 2019, an alternative single-pixel based approach was proposed in [131], which relies on the differential evolution algorithm and achieved a high successful-misguiding rate by only modifying less than 5 image pixels. In contrast, the decision-based attacks rely only on the class decision made by the targeted networks and does not require any knowledge regarding gradients or probabilities. This last category of adversarial attacks includes the *boundary attack* [132], the *noise attack*, and the *blur attack* (for images only) [124].

In the following, we will concentrate on the application of adversarial attacks in radar ATR. In [133], Huang et al. proposed four algorithms to misguide multi-layer perceptron (MLP) and CNN designed for radar ATR using HRRP. Two of them are fine-grained perturbations (i.e. the adversarial sample to be updated according to the input), while the other two are universal perturbations (i.e. image-agnostic). These algorithms and their main features are summarized in TABLE 7. Simulation results show that the proposed algorithms are highly aggressive when conducting both white and black attacks. In [134], Huang et al. considered the problem of adversarial attacks on radar ATR using SAR images. First, the I-FGSM was employed to generate adversarial examples for white-box and black-box nontargeted attacks on three classic CNN models: AlexNet, VGGNet, and ResNet. After that, the *ILCM* algorithm and the DBA algorithm were

TABLE 7. Adversarial attacks on ATR.

Reference	Name	Adversary's knowledge	Adversary's specificity	Main features
Huang et al. [133]	Algorithm-1	White-box & black-box	Nontargeted	Fine-grained perturbation; Fast gradient sign method (FGSM) variant with scaling factor obtained via binary search; more effective than FGSM
	Algorithm-2		Targeted	Fine-grained perturbation; multi-iteration method continuously updating
	Algorithm-3		Nontargeted	Universal perturbation via the aggregation of fine-grained perturbations
	Algorithm-4		Targeted	Universal perturbation by scaling one fine-grained perturbation
Huang et al. [134]	I-FGSM	White-box Black-box	Nontargeted	FGSM variant; in each iteration, the clipping function changes only 1 pixel
	ILCM		Targeted	Iteratively maximize the probability of specific false target class with lowest confidence score for clean image
	Decision based attack			Attack decisions; don't need gradients; find the decision boundary between clear sample and samples of desired false class
Lewis et al. [135]	FGSM	White-box	Nontargeted	Compute the gradient of loss function & seek the minimum step size to obtain adversarial sample
	DeepFool			Compute minimum distance to class boundary assuming linear classifier
	NewtonFool			Compute the minimum distance to a point x' adjacent to x so that the probability of x' belongs to true class of x approaches zero
	BIM			Maximize the loss along small steps in the gradient direction
	PGD			Maximize probability of some specific target class which is unlikely to be the true class for a given sample; multiple iterations
Wang et al. [136]	UAP	Black-box		Universal perturbation proposed in [137] is added to MSTAR images to fool CNNs; success rate higher than 80%
Wagner et al. [138]	DeepFool	White-box		Competitive Overcomplete Output Layer (COOL) used as the output layer to improve robustness against DeepFool

used to create adversarial examples for targeted white-box and black-box attack, respectively. The characteristics of these three algorithms are briefly introduced in TABLE 7. Simulation results show that using the adversarial examples generated with the I-FGSM, the success rate of VGGNet and ResNet in target recognition dropped from 95% to 7% when black-box attack was conducted. In addition, under the targeted white-box attack from ILCM, the confidence level of ResNet for the true class label decreased from 99% to 61.4%. Meanwhile, under the targeted black-box attack from decision-based attack, the confidence levels of AlexNet, VGGNet, and ResNet for the true class label were as low as 22.4%, 15.9%, and 23.2%, respectively. In [135], Lewis *et al.* tested five white-box adversarial attacks to fool the DL-based radar classifier: FGSM, DeepFool, NewtonFool, BIM, and PGD. In [136], the nontargeted black-box universal adversarial perturbation (UAP) was employed to fool the CNNs, for which the success rate in misguiding the network was higher than 80%.

As was mentioned before, although the mainstream research in the field of adversarial examples aims to “attack”, a considerable number of researchers work on the “defence” side, i.e. to improve the robustness of the DNNs to adversarial examples via adversarial training, adversarial detection, gradient-masking, etc. For example, in [138], the competitive overcomplete output layer (COOL) was designed to replace the commonly used softmax layer for improved robustness of the CNN against the adversarial examples generated by DeepFool.

V. DL FOR RADAR INTERFERENCE SUPPRESSION

Jamming and clutter are two types of interferences that limit the performance of modern radar systems. In this section, various DL-based jamming recognition and anti-jamming algorithms are reviewed. The technical trends in using the DNNs to address the challenging problem of marine target detection in sea clutter are also discussed.

A. JAMMING

In [145]–[151], various DNNs were designed for jamming signal classification, with the majority of them being CNNs. The main features of these networks are summarized in TABLE 8, along with the types of jamming signals that have been used for network training and performance testing. Specifically, In [146] and [147], an improved Siamese-CNN (S-CNN) was proposed, which is composed of two 1-D CNNs for feature extraction from the real and the imaginary parts of the data, respectively. This network only needs 500 training samples for each target class, and its performance were compared with various machine learning methods (e.g. the SVM). In [148] and [149], the 1-D jamming signals were transformed to 2-D time-frequency images via time frequency analysis so that they could be processed with CNN. In [149], a DNN based on the bilinear EfficientNet-B3 and the attention mechanism was proposed. The model parameters of EfficientNet-B3 obtained in the pretraining process using the ImageNet dataset were used as the initial weights of the proposed network. Note that EfficientNet-B3 belongs to a large family of EfficientNet algorithms (named as EfficientNet-B0 to B7) [150]. Although the accuracy of EfficientNet-B3 is 4% lower than that of EfficientNet-B7, the amount of model parameters involved in the former is only 1/5 of the latter, which indicates less training time. In [151], a VGG-16 variant was developed for barrage jamming detection and classification for SAR, where the statistical characteristics of SAR echo signals was exploited.

Except for the works discussed above, using the DL-based approaches to perform target classification in the presence of jamming [152], to choose the optimum anti-jamming strategy for radar [153], [154], to analyze the probability of radar being jammed [155], and to adaptively select the best method to jam an enemy radar [157] have also been investigated. The DNN structures proposed in these works and their distinctive features are summarized in TABLE 8. Finally, a detailed discussion regarding the application of artificial intelligence

TABLE 8. DL for jamming recognition and suppression.

Reference	Objective	DNN structure	Main features	Type of jamming
Mendoza et al. [145]	Jamming signal classification	12-layer neural network (NN)	<input type="checkbox"/> Proved that NN using power spectrum samples outperforms the one using autocorrelation	(1); (5) (LFM & power-law FM);
Shao et al. [146][147]		Improved Siamese-CNN: two 1-D CNN ($4 \times \text{Conv} + 1 \times \text{FC}$) to extract features of real & imaginary data	<input type="checkbox"/> Work with limited training samples (500/class) <input type="checkbox"/> Performance compared with various machine learning methods, e.g. SVM, 1D-CNN, etc.	12 types (1)-(9); (2)+(9); (7)+(8); (3)+(6)
Liu et al. [148]		CNN ($4 \times \text{Conv} + 4 \times \text{POOL} + 1 \times \text{FC}$)	<input type="checkbox"/> Preprocessing: normalization, filtering, STFT, adaptive cropping of the time-frequency map <input type="checkbox"/> Jamming detection (OS-CFAR) & measurement	(2); (7); (10)-(16)
Xiao et al. [149]		Bilinear EfficientNet-B3 + attention mechanism + transfer learning	<input type="checkbox"/> Preprocessing: time-frequency analysis <input type="checkbox"/> Attention mechanism + transfer learning	(2); (10); (11); (12); (14); (15); (20)
Yu et al. [151]		CNN (VGG16 variant, 13 layers)	<input type="checkbox"/> Statistical characteristics of SAR echo is exploited	Barrage ((17)-(19))
Wang et al. [152]	Target classification with jamming present	Stacked sparse autoencoder	<input type="checkbox"/> Polluted-spectrum recovery via compressed sensing <input type="checkbox"/> Three types of airplanes are classified based on micro-Doppler effects	(1)
Li et al. [153][154]	Anti-jamming strategy for radar	Actor-critic style: MLP ($3 \times \text{FC}$); CNN ($2 \times \text{Conv} + 1 \times \text{FC}$); LSTM ($1 \times \text{LSTM} + 2 \times \text{FC}$)	<input type="checkbox"/> Frequency agile radar employing deception sub-pulses to mislead the jammer <input type="checkbox"/> Anti mainlobe jamming	Barrage/spot jamming
Ak et al. [155]	Analyze probability of radar being jammed	<input type="checkbox"/> Double deep-Q network (3 hidden layers) <input type="checkbox"/> LSTM: 32 hidden units	<input type="checkbox"/> Reinforcement learning with knowledge-based random-access agent (KARA) strategy and least aggregate reward agent (LARA) strategy	Jammer channel hopping dynamics generated by Markov mechanism
Hong et al. [156]	Radar signal recognition & jamming prediction	CNN	<input type="checkbox"/> Radar signals with 6 types of RF modulation and 7 types of PRI modulation are considered	Varies based on radar signal under consideration
Pietro et al. [157]		1. Deep neural network: 4 hidden layers 2. LSTM: ($2 \times \text{LSTM} + 1 \times \text{FC}$)	<input type="checkbox"/> Adaptive jamming methods selection for unknown radar signals	

(1) pure noise; (2) interrupted sampling repeater jamming (ISRJ); (3) aiming; (4) blocking; (5) sweeping; (6) distance deception; (7) dense false targets; (8) smart noise; (9) chaff; (10) noise amplitude modulation jamming (AM); (11) noise frequency modulation jamming (FM); (12) noise convolution jamming (CN); (13) noise product jamming (CP); (14) smeared spectrum jamming (SMSP); (15) chopping and interleaving jamming (C&I); (16) comb spectral jamming (COMB); (17) single frequency; (18) narrowband barrage; (19) wideband barrage; (20) rectangular wave convolution jamming;

in electronic warfare systems was presented in [158], which is also recommended for readers who are interested in the recent trends of DL-based jamming/anti-jamming techniques.

B. CLUTTER

Marine target detection is a much more challenging task for radar than ground moving target detection due to the highly nonhomogeneous and time-varying clutter incurred by the sea. An early attempt of using machine learning methods for target detection in the presence of sea clutter was made in [159], where k-Nearest-Neighbor and SVM were used for marine target/clutter classification using the data collected by the S-band NetRAD system jointly developed by the University College London and the University of Cape Town [160].

With DL gaining popularity in recent years, many researchers resort to DNNs to further improve the detection performance of marine radars [161]–[164]. Specifically, in [161], Pan *et al.* used the Faster R-CNN proposed by Ren *et al.* in [104] for target detection using the sea clutter dataset collected with the X-band ground-based Fynmeet marine radar by the council for scientific and industrial research (CSIR). In [162], Chen *et al.* proposed a dual-channel convolutional neural network (DCCNN) made of LeNet and VGG16, for which the amplitude and the time-frequency information were used as two inputs, and the features extracted from the two channels were fused at the FC layer. One distinctive characteristic of [162] is that softmax classifier with variable threshold and SVM classifier with controllable false alarm rates were designed. The performance of the proposed network was tested with two datasets,

the Intelligent PIXel processing radar (IPIX) dataset collected by the fully coherent dual-pol X-band radar for *floating target* and the CSIR dataset for *maneuvering marine target*. In [163], a fully convolutional network (FCC) with 20 layers were proposed for ship detection in SAR images collected by Gaofen-3 and TerraSAR-X. It is worth mentioning that pixel truncation was implemented as a preprocessing procedure assuming that the potential ship pixels are brighter than the clutter, which is not necessarily true. Finally, in [164], a DL-based empirical clutter model named as the multi-source input neural network (MSINN) was proposed to predict the sea clutter reflectively. This model was tested with the sea clutters collected by ground-based UHF band polarized radar and was proven to fit the measurement data better than the existing empirical sea clutter models.

Although most research papers in this field focus on sea clutter, DNNs have also been designed to address other types of clutter. For example, in [165], Cifola *et al.* considered the problem of clutter/target recognition for drone signals polluted by wind turbine returns. A denoising adversarial autoencoder was designed, the performance of which was tested with the micro-Doppler signatures of drones and wind-turbines measured with X-band CW radar. In [166], Lepetit *et al.* used U-Net, a CNN variant that was originally proposed for medical image segmentation, to remove clutter from precipitation echoes collected by weather radar. 150,000 images collected by the Trappes polarimetric ground weather radar in Météo-France were used for network training.

The DNN structures presented in [161]–[166] and their main features are summarized in TABLE 9. Note that

TABLE 9. DL for clutter estimation and suppression.

Reference	Objective	DNN structure	Main features
Pan et al. [161]	Marine target detection in presence of sea clutter	Faster R-CNN	<input type="checkbox"/> Network is initialized with VGG16 pre-trained model & trained with alternative training (RPN --- fast R-CNN ---- RPN)
Chen et al. [162]		Dual-channel CNN: LeNet + VGG16	<input type="checkbox"/> Amplitude and time-frequency information are used as two inputs for dual-channel network <input type="checkbox"/> Variable threshold softmax classifier & false alarm controllable classifier SVM
An et al. [163]		FCN: $10 \times \text{Conv}, 5 \times \text{POOL}, 3 \times \text{Deconv}$	<input type="checkbox"/> Preprocessing: pixel truncation assuming potential ship pixels are brighter than clutter <input type="checkbox"/> Iterative censoring scheme for detection <input type="checkbox"/> CFAR detector designed assuming Rayleigh & K clutter model
Ma et al. [164]	Sea clutter reflectivity prediction with empirical clutter model	Muti-source input neural network	<input type="checkbox"/> Preprocessing: determine sea clutter effective region using yolov3-tiny model <input type="checkbox"/> MSINN clutter model for Yellow Sea, China
Cifola et al. [165]	Separation of drone signals from wind turbine clutter	Denoising adversarial autoencoder: discriminator ($6 \times \text{Conv}$) + autoencoder	<input type="checkbox"/> Autoencoder trained to reconstruct spectrogram containing drone-only signal <input type="checkbox"/> Discriminator is used to distinguish drone-only signal from clutter
Lepetit et al. [166]	Clutter removal from echoes collected by weather radar	U-net	<input type="checkbox"/> Two sets of data used: weather-plus-clutter images & clutter-only images (clean images not required for training)

except for the works mentioned above, deep convolutional autoencoders were proposed for target detection in sea clutter in [167], [168], and a LSTM-based network was designed for sea clutter prediction in [169]. Since these networks were tested only with simulated data, they are expected to exhibit noticeable performance degradation in real-life detection scenarios.

VI. CONCLUSION

In this work, we consider the application of DL algorithms in radar signal processing. With the DL gaining popularity rapidly in recent years, DL for radar signal recognition, DL for ATR based on HRRP/Doppler signatures/SAR images, and DL for radar jamming recognition & clutter suppression have been explored thoroughly by many researchers. Although classification accuracies of 98%-100% have been reported in many research works on radar ATR with DL networks using the MSTAR dataset, it should be emphasized that there is a long way to go before the DL approaches become qualified substitutes for the classic radar ATR methods. Firstly, DL networks demand large amount of training data. Unlike the typical problem of image classification, for which large amounts of training data are available online, representative real-world HRRPs and SAR images that are labelled with accurately verified targets are simply not readily available for everyone at demand. Not to mention that a network trained under a specific environment doesn't work the same way when the environment changes. Secondly, although some DL networks reach high accuracies with limited training data, most of them were tested with only the MSTAR dataset, which has also been used to prove the high -accuracy performance (above 97%) of traditional machine learning based ATR methods 20 years ago. Moreover, the ever-evolving adversarial attacks also post great security risk to the DNNs. This work provides a full picture of numerous potential research opportunities and grave challenges in applying the DL-based approaches to address the existing problems in radar signal processing, which serves as a good reference work for researchers interested in this field.

ACKNOWLEDGMENT

The authors would like to thank the anonymous reviewers for their insightful comments and suggestions, which definitely made the work more technically sound.

REFERENCES

- [1] E. Mason, B. Yonet, and B. Yazici, "Deep learning for radar," in *Proc. IEEE Radar Conf. (RadarConf)*, May 2017, pp. 1703–1708.
- [2] F. Gini, "Grand challenges in radar signal processing," *Frontiers Signal Process.*, vol. 1, pp. 1–6, Mar. 2021.
- [3] P. Lang, X. Fu, M. Martorella, J. Dong, R. Qin, X. Meng, and M. Xie, "A comprehensive survey of machine learning applied to radar signal processing," 2020, *arXiv:2009.13702*. [Online]. Available: <https://arxiv.org/abs/2009.13702>
- [4] X. X. Zhu, D. Tuia, L. Mou, G.-S. Xia, L. Zhang, F. Xu, and F. Fraundorfer, "Deep learning in remote sensing: A comprehensive review and list of resources," *IEEE Geosci. Remote Sens. Mag.*, vol. 5, no. 4, pp. 8–36, Dec. 2017.
- [5] L. Zhang, L. Zhang, and B. Du, "Deep learning for remote sensing data: A technical tutorial on the state of the art," *IEEE Geosci. Remote Sens. Mag.*, vol. 4, no. 2, pp. 22–40, Jun. 2016.
- [6] S. Haykin, "Cognitive radar: A way of the future," *IEEE Signal Process. Mag.*, vol. 23, no. 1, pp. 30–40, Jan. 2006.
- [7] G. E. Smith and T. J. Reininger, "Reinforcement learning for waveform design," in *Proc. IEEE Radar Conf. (RadarConf)*, May 2021, pp. 1–6.
- [8] C. E. Thornton, R. M. Buehrer, A. F. Martone, and K. D. Sherbondy, "Experimental analysis of reinforcement learning techniques for spectrum sharing radar," in *Proc. IEEE Int. Radar Conf. (RADAR)*, Apr. 2020, pp. 67–72.
- [9] C. E. Thornton, M. A. Kozy, R. M. Buehrer, A. F. Martone, and K. D. Sherbondy, "Deep reinforcement learning control for radar detection and tracking in congested spectral environments," *IEEE Trans. Cognit. Commun. Netw.*, vol. 6, no. 4, pp. 1335–1349, Dec. 2020.
- [10] Army Fast-Tracks Adaptable Radars for Congested Environments, Defense Insider, U. S. Army DEVCOM Army Res. Lab. Public Affairs, Adelphi, MD, USA, 2020.
- [11] M. Kozy, J. Yu, R. M. Buehrer, A. Martone, and K. Sherbondy, "Applying deep-Q networks to target tracking to improve cognitive radar," in *Proc. IEEE Radar Conf. (RadarConf)*, Apr. 2019, pp. 1–6.
- [12] H. Deng, B. Himed, and Z. Geng, "Mimo radar waveform design for transmit beamforming and orthogonality," *IEEE Trans. Aerosp. Electron. Syst.*, vol. 52, no. 3, pp. 1421–1433, Jun. 2016.
- [13] J. Hu, Z. Wei, Y. Li, H. Li, and J. Wu, "Designing unimodular waveform(s) for MIMO radar by deep learning method," *IEEE Trans. Aerosp. Electron. Syst.*, vol. 57, no. 2, pp. 1184–1196, Apr. 2021.
- [14] W. Zhang, J. Hu, Z. Wei, H. Ma, X. Yu, and H. Li, "Constant modulus waveform design for MIMO radar transmit beampattern with residual network," *Signal Process.*, vol. 177, Dec. 2020, Art. no. 107735.

- [15] K. Zhong, W. Zhang, Q. Zhang, J. Hu, P. Wang, X. Yu, and Q. Zhou, “MIMO radar waveform design via deep learning,” in *Proc. IEEE Radar Conf. (RadarConf)*, May 2021, pp. 1–5.
- [16] L. Wang, S. Fortunati, M. S. Greco, and F. Gini, “Reinforcement learning-based waveform optimization for MIMO multi-target detection,” in *Proc. 52nd Asilomar Conf. Signals, Syst., Comput.*, Oct. 2018, pp. 1329–1335.
- [17] J. M. Kurdzo, J. Y. N. Cho, B. L. Cheong, and R. D. Palmer, “A neural network approach for waveform generation and selection with multi-mission radar,” in *Proc. IEEE Radar Conf. (RadarConf)*, Apr. 2019, pp. 1–6.
- [18] A. M. Elbir, K. V. Mishra, and Y. C. Eldar, “Cognitive radar antenna selection via deep learning,” *IET Radar, Sonar Navigat.*, vol. 13, pp. 871–880, Jun. 2019.
- [19] Z. Geng, H. Deng, and B. Himed, “Interference mitigation for airborne MIMO radar,” in *Proc. Int. Conf. Radar Syst. (Radar)*, 2017, pp. 1–6.
- [20] T. Cheng, B. Wang, Z. Wang, R. Dong, and B. Cai, “Lightweight CNNs-based interleaved sparse array design of phased-MIMO radar,” *IEEE Sensors J.*, vol. 21, no. 12, pp. 13200–13214, Jun. 2021.
- [21] C. Wang, J. Wang, and X. Zhang, “Automatic radar waveform recognition based on time-frequency analysis and convolutional neural network,” in *Proc. IEEE Int. Conf. Acoust., Speech Signal Process. (ICASSP)*, Mar. 2017, pp. 2437–2441.
- [22] R. Zhou, F. Liu, and C. W. Gravelle, “Deep learning for modulation recognition: A survey with a demonstration,” *IEEE Access*, vol. 8, pp. 67366–67376, 2020.
- [23] P. Itkin and N. Levanon, “Ambiguity function based radar waveform classification and unsupervised adaptation using deep CNN models,” in *Proc. IEEE Int. Conf. Microw., Antennas, Commun. Electron. Syst. (COMCAS)*, Nov. 2019, pp. 1–6.
- [24] A. Dai, H. Zhang, and H. Sun, “Automatic modulation classification using stacked sparse auto-encoders,” in *Proc. IEEE 13th Int. Conf. Signal Process. (ICSP)*, Chengdu, China, Nov. 2016, pp. 248–252.
- [25] Z. Qu, W. Wang, C. Hou, and C. Hou, “Radar signal intra-pulse modulation recognition based on convolutional denoising autoencoder and deep convolutional neural network,” *IEEE Access*, vol. 7, pp. 112339–112347, 2019.
- [26] K. Ren, H. Ye, G. Gu, and Q. Chen, “Pulses classification based on sparse auto-encoders neural networks,” *IEEE Access*, vol. 7, pp. 92651–92660, 2019.
- [27] X. Li, Z. Liu, Z. Huang, and W. Liu, “Radar emitter classification with attention-based multi-RNNs,” *IEEE Commun. Lett.*, vol. 24, no. 9, pp. 2000–2004, Sep. 2020.
- [28] X. Li, Z. Liu, and Z. Huang, “Attention-based radar PRI modulation recognition with recurrent neural networks,” *IEEE Access*, vol. 8, pp. 57426–57436, 2020.
- [29] Z.-M. Liu and P. S. Yu, “Classification, denoising, and deinterleaving of pulse streams with recurrent neural networks,” *IEEE Trans. Aerosp. Electron. Syst.*, vol. 55, no. 4, pp. 1624–1639, Aug. 2019.
- [30] S.-H. Kong, M. Kim, L. M. Hoang, and E. Kim, “Automatic LPI radar waveform recognition using CNN,” *IEEE Access*, vol. 6, pp. 4207–4219, 2018.
- [31] J. Wan, X. Yu, and Q. Guo, “LPI radar waveform recognition based on CNN and TPOT,” *Symmetry*, vol. 11, no. 5, p. 725, May 2019.
- [32] Z. Ma, Z. Huang, A. Lin, and G. Huang, “LPI radar waveform recognition based on features from multiple images,” *Sensors*, vol. 20, no. 2, p. 526, Jan. 2020.
- [33] B. Lay and A. Charlish, “Classifying LPI signals with transfer learning on CNN architectures,” in *Proc. Sensor Signal Process. Defence Conf. (SSPD)*, Sep. 2020, pp. 1–5.
- [34] Q. Guo, X. Yu, and G. Ruan, “LPI radar waveform recognition based on deep convolutional neural network transfer learning,” *Symmetry*, vol. 11, no. 4, p. 540, Apr. 2019.
- [35] S. Zhang, A. Ahmed, and Y. D. Zhang, “Sparsity-based time-frequency analysis for automatic radar waveform recognition,” in *Proc. IEEE Int. Radar Conf. (RADAR)*, Apr. 2020, pp. 548–553.
- [36] X. Ni, H. Wang, F. Meng, J. Hu, and C. Tong, “LPI radar waveform recognition based on multi-resolution deep feature fusion,” *IEEE Access*, vol. 9, pp. 26138–26146, 2021.
- [37] Z. Pan, S. Wang, M. Zhu, and Y. Li, “Automatic waveform recognition of overlapping LPI radar signals based on multi-instance multi-label learning,” *IEEE Signal Process. Lett.*, vol. 27, pp. 1275–1279, 2020.
- [38] G. Ghadimi, Y. Norouzi, R. Bayderkhani, M. M. Nayebi, and S. M. Karbasi, “Deep learning-based approach for low probability of intercept radar signal detection and classification,” *J. Commun. Technol. Electron.*, vol. 65, no. 10, pp. 1179–1191, Oct. 2020.
- [39] S. Wei, Q. Qu, H. Su, J. Shi, X. Zeng, and X. Hao, “Intra-pulse modulation radar signal recognition based on squeeze- and excitation networks,” *Signal, Image Video Process.*, vol. 14, no. 6, pp. 1133–1141, Sep. 2020.
- [40] A. Orduyilmaz, E. Yar, M. B. Kocamis, M. Serin, and M. Efe, “Machine learning-based radar waveform classification for cognitive EW,” *Signal, Image Video Process.*, vol. 15, pp. 1–10, Apr. 2021.
- [41] A. Yildirim and S. Kiranyaz, “1D convolutional neural networks versus automatic classifiers for known LPI radar signals under white Gaussian noise,” *IEEE Access*, vol. 8, pp. 180534–180543, 2020.
- [42] Z. Geng, “Evolution of netted radar systems,” *IEEE Access*, vol. 8, pp. 124961–124977, 2020.
- [43] B. Yonel, E. Mason, and B. Yazici, “Deep learning for waveform estimation in passive synthetic aperture radar,” in *Proc. IEEE Radar Conf. (RadarConf)*, Apr. 2018, pp. 1395–1400.
- [44] B. Yonel, E. Mason, and B. Yazici, “Deep learning for waveform estimation and imaging in passive radar,” *IET Radar, Sonar Navigat.*, vol. 13, no. 6, pp. 915–926, Jun. 2019.
- [45] Q. Wang, P. Du, J. Yang, G. Wang, J. Lei, and C. Hou, “Transferred deep learning based waveform recognition for cognitive passive radar,” *Signal Process.*, vol. 155, pp. 259–267, Feb. 2019.
- [46] M. Stone. (Mar. 2020). *Why Adversarial Examples are Such a Dangerous Threat to Deep Learning*. Accessed: Jun. 23, 2021. [Online]. Available: <https://securityintelligence.com/articles/why-adversarial-examples-are-such-a-dangerous-threat-to-deep-learning/>
- [47] M. Sadeghi and E. G. Larsson, “Adversarial attacks on deep-learning based radio signal classification,” *IEEE Wireless Commun. Lett.*, vol. 8, no. 1, pp. 213–216, Feb. 2019.
- [48] S. Kokalj-Filipovic, R. Miller, N. Chang, and C. L. Lau, “Mitigation of adversarial examples in RF deep classifiers utilizing AutoEncoder pre-training,” in *Proc. Int. Conf. Mil. Commun. Inf. Syst. (ICMCIS)*, May 2019, pp. 1–6.
- [49] S. Kokalj-Filipovic, R. Miller, and G. Vanhoy, “Adversarial examples in RF deep learning: Detection and physical robustness,” in *Proc. IEEE Global Conf. Signal Inf. Process. (GlobalSIP)*, Nov. 2019, pp. 1–5.
- [50] B. Chen, H. Liu, J. Chai, and Z. Bao, “Large margin feature weighting method via linear programming,” *IEEE Trans. Knowl. Data Eng.*, vol. 21, no. 10, pp. 1475–1488, Oct. 2009.
- [51] B. Feng, L. Du, H.-W. Liu, and F. Li, “Radar HRRP target recognition based on K-SVD algorithm,” in *Proc. IEEE CIE Int. Conf. Radar*, Chengdu, China, Oct. 2011, pp. 642–645.
- [52] R. Alake. (Jul. 2020). *What AlexNet Brought to the World of Deep Learning*. Accessed: Sep. 18, 2021. [Online]. Available: <https://towardsdatascience.com/what-alexnet-brought-to-the-world-of-deep-learning46c7974b46fc>
- [53] Y. Ouali, C. Hudelot, and M. Tami, “An overview of deep semi-supervised learning,” 2020, *arXiv:2006.05278*. [Online]. Available: <https://arxiv.org/abs/2006.05278>
- [54] B. Feng, B. Chen, and H. Liu, “Radar HRRP target recognition with deep networks,” *Pattern Recognit.*, vol. 61, pp. 379–393, Jan. 2017.
- [55] M. Pan, J. Jiang, Q. Kong, J. Shi, Q. Sheng, and T. Zhou, “Radar HRRP target recognition based on t-SNE segmentation and discriminant deep belief network,” *IEEE Geosci. Remote Sens. Lett.*, vol. 14, no. 9, pp. 1609–1613, Sep. 2017.
- [56] C. Zhao, X. He, J. Liang, T. Wang, and C. Huang, “Radar HRRP target recognition via semi-supervised multi-task deep network,” *IEEE Access*, vol. 7, pp. 114788–114794, 2019.
- [57] B. Xu, B. Chen, J. Wan, H. Liu, and L. Jin, “Target-aware recurrent attentional network for radar HRRP target recognition,” *Signal Process.*, vol. 155, pp. 268–280, Feb. 2019.
- [58] B. Xu, B. Chen, J. Liu, and C. Du, “Gaussian mixture model-tensor recurrent neural network for HRRP target recognition,” in *Proc. Int. Radar Conf. (RADAR)*, Sep. 2019, pp. 1–6.
- [59] K. Liao, J. Si, F. Zhu, and X. He, “Radar HRRP target recognition based on concatenated deep neural networks,” *IEEE Access*, vol. 6, pp. 29211–29218, 2018.
- [60] C. Guo, Y. He, H. Wang, T. Jian, and S. Sun, “Radar HRRP target recognition based on deep one-dimensional residual-inception network,” *IEEE Access*, vol. 7, pp. 9191–9204, 2019.
- [61] J. Song, Y. Wang, W. Chen, Y. Li, and J. Wang, “Radar HRRP recognition based on CNN,” *J. Eng.*, vol. 2019, no. 21, pp. 7766–7769, Nov. 2019.

- [62] Y. Song, Y. Li, Y. Wang, and C. Hu, "Data augmentation for imbalanced HRRP recognition using deep convolutional generative adversarial network," *IEEE Access*, vol. 8, pp. 201686–201695, 2020.
- [63] J. Lunden and V. Koivunen, "Deep learning for HRRP-based target recognition in multistatic radar systems," in *Proc. IEEE Radar Conf. (RadarConf)*, May 2016, pp. 1–6.
- [64] O. Karabayir, O. M. Yucedag, M. Z. Kartal, and H. A. Serim, "Convolutional neural networks-based ship target recognition using high resolution range profiles," in *Proc. 18th Int. Radar Symp. (IRS)*, Jun. 2017, pp. 1–9.
- [65] W. Liu, G. Zhang, W. Chen, and C. Hang, "Radar hrrp target recognition based ON stacked frame maximum likelihood profile-trajectory similarity autoencoders," in *Proc. IEEE Int. Geosci. Remote Sens. Symp. (IGARSS)*, Jul. 2019, pp. 3748–3751.
- [66] L. Zhang, Y. Li, Y. Wang, J. Wang, and T. Long, "Polarimetric HRRP recognition based on ConvLSTM with self-attention," *IEEE Sensors J.*, vol. 21, no. 6, pp. 7884–7898, Mar. 2021.
- [67] L. Zhang, C. Han, Y. Wang, Y. Li, and T. Long, "Polarimetric HRRP recognition based on feature-guided transformer model," *Electron. Lett.*, vol. 57, no. 18, pp. 705–707, Aug. 2021.
- [68] H. Griffiths, A. Charlish, and N. Goodman, "Cognitive radar," STO, Neuilly-sur-Seine Cedex, France, Tech. Rep. AC/323(SET-227)TP/947, 2020.
- [69] Y. D. Dadon, S. Yamin, S. Feintuch, H. H. Permuter, I. Bilik, and J. Tabrikian, "Moving target classification based on micro-Doppler signatures via deep learning," in *Proc. IEEE Radar Conf. (RadarConf)*, May 2021, pp. 1–6.
- [70] Y. Yang, C. Hou, Y. Lang, T. Sakamoto, Y. He, and W. Xiang, "Omnidirectional motion classification with monostatic radar system using micro-Doppler signatures," *IEEE Trans. Geosci. Remote Sens.*, vol. 58, no. 5, pp. 3574–3587, May 2020.
- [71] E. A. Hadhrami, M. A. Mufti, B. Taha, and N. Werghi, "Ground moving radar targets classification based on spectrogram images using convolutional neural networks," in *Proc. 19th Int. Radar Symp. (IRS)*, Jun. 2018, pp. 1–9.
- [72] E. A. Hadhrami, M. A. Mufti, B. Taha, and N. Werghi, "Transfer learning with convolutional neural networks for moving target classification with micro-Doppler radar spectrograms," in *Proc. Int. Conf. Artif. Intell. Big Data (ICAIBD)*, May 2018, pp. 148–154.
- [73] E. Alhadhrami, M. Al-Mufti, B. Taha, and N. Werghi, "Learned micro-Doppler representations for targets classification based on spectrogram images," *IEEE Access*, vol. 7, pp. 139377–139387, 2019.
- [74] B. K. Kim, H.-S. Kang, and S.-O. Park, "Drone classification using convolutional neural networks with merged Doppler images," *IEEE Geosci. Remote Sens. Lett.*, vol. 14, no. 1, pp. 38–42, Jan. 2017.
- [75] S. Rahman and D. A. Robertson, "Classification of drones and birds using convolutional neural networks applied to radar micro-Doppler spectrogram images," *IET Radar, Sonar Navigat.*, vol. 14, no. 5, pp. 653–661, May 2020.
- [76] G. J. Mendis, J. Wei, and A. Madanayake, "Deep learning cognitive radar for micro UAS detection and classification," in *Proc. Cognit. Commun. Aerosp. Appl. Workshop (CCAA)*, Jun. 2017, pp. 1–5.
- [77] G. J. Mendis, T. Randeny, J. Wei, and A. Madanayake, "Deep learning based Doppler radar for micro UAS detection and classification," in *Proc. IEEE Mil. Commun. Conf. (MILCOM)*, Nov. 2016, pp. 924–929.
- [78] S. Samaras, E. Diamantidou, D. Ataloglou, N. Sakellariou, A. Vafeiadis, V. Magoulianitis, A. Lalas, A. Dimou, D. Zarpalias, K. Votis, P. Daras, and D. Tzovaras, "Deep learning on multi sensor data for counter UAV applications—A systematic review," *Sensors*, vol. 19, no. 22, p. 4837, Nov. 2019.
- [79] U. K. Majumder, E. P. Blasch, D. A. Garren, *Deep Learning for Radar and Communications Automatic Target Recognition*. Boston, MA, USA: Artech House, 2020.
- [80] K. R. S. Rosenbach, "ATR of battlefield targets by SAR classification results using the public MSTAR dataset compared with a dataset by QinetiQ, U.K.," in *Proc. RTO Sensors Electron. Technol. Panel Symp.*, 2004, pp. 1–12.
- [81] R. Schumacher and J. Schiller, "Non-cooperative target identification of battlefield targets—classification results based on SAR images," in *Proc. IEEE Int. Radar Conf.*, May 2005, pp. 167–172.
- [82] S. Chen, H. Wang, F. Xu, and Y.-Q. Jin, "Target classification using the deep convolutional networks for SAR images," *IEEE Trans. Geosci. Remote Sens.*, vol. 54, no. 8, pp. 4806–4817, Aug. 2016.
- [83] J. Pei, Y. Huang, W. Huo, Y. Zhang, J. Yang, and T.-S. Yeo, "SAR automatic target recognition based on multiview deep learning framework," *IEEE Trans. Geosci. Remote Sens.*, vol. 56, no. 4, pp. 2196–2210, Apr. 2018.
- [84] H. Furukawa, "Deep learning for end-to-end automatic target recognition from synthetic aperture radar imagery," *IEICE Tech. Rep.*, vol. 117, no. 403, pp. 35–40, Jan. 2018.
- [85] R. Shang, J. Wang, L. Jiao, R. Stolkin, B. Hou, and Y. Li, "SAR targets classification based on deep memory convolution neural networks and transfer parameters," *IEEE J. Sel. Topics Appl. Earth Observ. Remote Sens.*, vol. 11, no. 8, pp. 2834–2846, Aug. 2018.
- [86] F. Zhou, L. Wang, X. Bai, and Y. Hui, "SAR ATR of ground vehicles based on LM-BN-CNN," *IEEE Trans. Geosci. Remote. Sens.*, vol. 56, no. 12, pp. 7282–7293, Dec. 2018.
- [87] S. A. Wagner, "SAR ATR by a combination of convolutional neural network and support vector machines," *IEEE Trans. Aerosp. Electron. Syst.*, vol. 52, no. 6, pp. 2861–2872, Dec. 2016.
- [88] S. Wagner, K. Barth, and S. Bruggenwirth, "A deep learning SAR ATR system using regularization and prioritized classes," in *Proc. IEEE Radar Conf. (RadarConf)*, May 2017, pp. 772–777.
- [89] L. Kaiser, O. Nachum, A. Roy, and S. Bengio, "Learning to remember rare events," in *Proc. 5th Int. Conf. Learn. Represent.*, 2017, pp. 1–10.
- [90] R. Xue, X. Bai, and F. Zhou, "Spatial-temporal ensemble convolution for sequence SAR target classification," *IEEE Trans. Geosci. Remote Sens.*, vol. 59, no. 2, pp. 1250–1262, Feb. 2021.
- [91] F. Zhang, C. Hu, Q. Yin, W. Li, H.-C. Li, and W. Hong, "Multi-aspect-aware bidirectional LSTM networks for synthetic aperture radar target recognition," *IEEE Access*, vol. 5, pp. 26880–26891, 2017.
- [92] X. Bai, R. Xue, L. Wang, and F. Zhou, "Sequence SAR image classification based on bidirectional convolution-recurrent network," *IEEE Trans. Geosci. Remote Sens.*, vol. 57, no. 11, pp. 9223–9235, Nov. 2019.
- [93] J. Pearl, "Theoretical impediments to machine learning with seven sparks from the causal revolution," 2018, *arXiv:1801.04016*. [Online]. Available: <https://arxiv.org/abs/1801.04016>
- [94] B. Pei and Z. Bao, "Multi-aspect radar target recognition method based on scattering centers and HMMs classifiers," *IEEE Trans. Aerosp. Electron. Syst.*, vol. 41, no. 3, pp. 1067–1074, Jul. 2005.
- [95] S. Deng, L. Du, C. Li, J. Ding, and H. Liu, "SAR automatic target recognition based on Euclidean distance restricted autoencoder," *IEEE J. Sel. Topics Appl. Earth Observ. Remote Sens.*, vol. 10, no. 7, pp. 3323–3333, Jul. 2017.
- [96] J. Geng, J. Fan, H. Wang, X. Ma, B. Li, and F. Chen, "High-resolution SAR image classification via deep convolutional autoencoders," *IEEE Trans. Geosci. Remote Sens.*, vol. 12, no. 11, pp. 2351–2355, Nov. 2015.
- [97] J. Geng, H. Wang, J. Fan, and X. Ma, "Deep supervised and contractive neural network for SAR image classification," *IEEE Trans. Geosci. Remote Sens.*, vol. 55, no. 4, pp. 2442–2459, Apr. 2017.
- [98] G. Dong, G. Liao, H. Liu, and G. Kuang, "A review of the autoencoder and its variants: A comparative perspective from target recognition in synthetic-aperture radar images," *IEEE Geosci. Remote Sens. Mag.*, vol. 6, no. 3, pp. 44–68, Sep. 2018.
- [99] J. Guo, L. Wang, D. Zhu, and C. Hu, "Compact convolutional autoencoder for SAR target recognition," *IET Radar, Sonar Navigat.*, vol. 14, no. 7, pp. 967–972, Jul. 2020.
- [100] C. P. Schwegmann, W. Kleynhans, B. P. Salmon, L. W. Mdakane, and R. G. Meyer, "Synthetic aperture radar ship detection using capsule networks," in *Proc. IEEE Int. Geosci. Remote Sens. Symp. (IGARSS)*, Jul. 2018, pp. 725–728.
- [101] L. De Laurentiis, A. Pomente, F. Del Frate, and G. Schiavon, "Capsule and convolutional neural network-based SAR ship classification in sentinel-1 data," *Proc. SPIE*, vol. 11154, Oct. 2019, Art. no. 1115405.
- [102] R. Shah, A. Soni, V. Mall, T. Gadhiya, and A. K. Roy, "Automatic target recognition from SAR images using capsule networks," in *Pattern Recognition and Machine Intelligence*. Cham, Switzerland: Springer, 2019, pp. 377–386.
- [103] J. Ding, L. Wen, C. Zhong, and O. Loffeld, "Video SAR moving target indication using deep neural network," *IEEE Trans. Geosci. Remote Sens.*, vol. 58, no. 10, pp. 7194–7204, Mar. 2020.
- [104] S. Ren, K. He, R. Girshick, and J. Sun, "Faster R-CNN: Towards real-time object detection with region proposal networks," *IEEE Trans. Pattern Anal. Mach. Intell.*, vol. 39, no. 6, pp. 1137–1149, Jun. 2017.
- [105] K. El-Darymli, E. W. Gill, P. McGuire, D. Power, and C. Moloney, "Automatic target recognition in synthetic aperture radar imagery: A state-of-the-art review," *IEEE Access*, vol. 4, pp. 6014–6058, 2016.

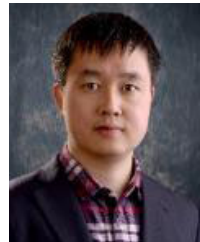
- [106] C. Clemente, L. Pallotta, D. Gaglione, A. De Maio, and J. J. Soraghan, "Automatic target recognition of military vehicles with Krawtchouk moments," *IEEE Trans. Aerosp. Electron. Syst.*, vol. 53, no. 1, pp. 493–500, Feb. 2017.
- [107] B. Hou, L. Wang, Q. Wu, Q. Han, and L. Jiao, "Complex Gaussian–Bayesian online dictionary learning for SAR target recognition with limited labeled samples," *IEEE Access*, vol. 7, pp. 120626–120637, 2019.
- [108] C. Wang, H. Gu, and W. Su, "SAR image classification using contrastive learning and pseudo-labels with limited data," *IEEE Geosci. Remote Sens. Lett.*, early access, Apr. 2, 2021, doi: 10.1109/LGRS.2021.3069224.
- [109] F. Zhang, Y. Wang, J. Ni, Y. Zhou, and W. Hu, "SAR target small sample recognition based on CNN cascaded features and AdaBoost rotation forest," *IEEE Geosci. Remote Sens. Lett.*, vol. 17, no. 6, pp. 1008–1012, Jun. 2020.
- [110] Z. Huang, Z. Pan, and B. Lei, "Transfer learning with deep convolutional neural network for SAR target classification with limited labeled data," *Remote Sens.*, vol. 9, no. 9, p. 907, 2017.
- [111] C. Zhong, X. Mu, X. He, J. Wang, and M. Zhu, "SAR target image classification based on transfer learning and model compression," *IEEE Geosci. Remote Sens. Lett.*, vol. 16, no. 3, pp. 412–416, Mar. 2019.
- [112] J. Ding, B. Chen, H. Liu, and M. Huang, "Convolutional neural network with data augmentation for SAR target recognition," *IEEE Geosci. Remote Sens. Lett.*, vol. 13, no. 3, pp. 364–368, Mar. 2016.
- [113] Q. Yu, H. Hu, X. Geng, Y. Jiang, and J. An, "High-performance SAR automatic target recognition under limited data condition based on a deep feature fusion network," *IEEE Access*, vol. 7, pp. 165646–165658, 2019.
- [114] Y. Kwak, W.-J. Song, and S.-E. Kim, "Speckle-noise-invariant convolutional neural network for SAR target recognition," *IEEE Geosci. Remote Sens. Lett.*, vol. 16, no. 4, pp. 549–553, Apr. 2019.
- [115] B. Lewis, T. Scarnati, E. Sudkamp, J. Nehrbass, S. Rosencrantz, and E. Zelnio, "A SAR dataset for ATR development: The synthetic and measured paired labeled experiment (SAMPLE)," *Proc. SPIE*, vol. 10987, pp. 39–54, May 2019.
- [116] T. Scarnati and B. Lewis, "A deep learning approach to the synthetic and measured paired and labeled experiment (SAMPLE) challenge problem," *Proc. SPIE*, vol. 10987, pp. 29–38, May 2019.
- [117] M. Cha, A. Majumdar, H. T. Kung, and J. Barber, "Improving SAR automatic target recognition using simulated images under deep residual refinements," in *Proc. IEEE Int. Conf. Acoust., Speech Signal Process. (ICASSP)*, Apr. 2018, pp. 2606–2610.
- [118] H. Zhu, R. Leung, and M. Hong, "Shadow compensation for synthetic aperture radar target classification by dual parallel generative adversarial network," *IEEE Sensors Lett.*, vol. 4, no. 8, pp. 1–4, Aug. 2020.
- [119] Z. Huang, Z. Pan, and B. Lei, "What, where, and how to transfer in SAR target recognition based on deep CNNs," *IEEE Trans. Geosci. Remote Sens.*, vol. 58, no. 4, pp. 2324–2336, Apr. 2020.
- [120] C. He, D. Xiong, Q. Zhang, and M. Liao, "Parallel connected generative adversarial network with quadratic operation for SAR image generation and application for classification," *Sensors*, vol. 19, no. 4, p. 871, Feb. 2019.
- [121] Q. An, Z. Pan, H. You, and Y. Hu, "Transitive transfer learning-based anchor free rotatable detector for SAR target detection with few samples," *IEEE Access*, vol. 9, pp. 24011–24025, 2021.
- [122] C. Lu and W. Li, "Ship classification in high-resolution SAR images via transfer learning with small training dataset," *Sensors*, vol. 19, no. 1, p. 63, Dec. 2018.
- [123] Y. Guo, L. Du, D. Wei, and C. Li, "Robust SAR automatic target recognition via adversarial learning," *IEEE J. Sel. Topics Appl. Earth Observ. Remote Sens.*, vol. 14, pp. 716–729, 2021.
- [124] J. Rauber, W. Brendel, and M. Bethge, " Foolbox: A Python toolbox to benchmark the robustness of machine learning models," in *Proc. Reliable Mach. Learn. Wild Workshop 34th Int. Conf. Mach. Learn.*, Sydney, NSW, Australia, 2017, pp. 1–6.
- [125] S. Haldar. (Apr. 9, 2020). *Gradient-Based Adversarial Attacks: An Introduction*. Accessed: Aug. 1, 2021. [Online]. Available: <https://medium.com/swlh/gradient-based-adversarial-attacks-an-introduction-526238660dc9>
- [126] I. J. Goodfellow, J. Shlens, and C. Szegedy, "Explaining and harnessing adversarial examples," in *Proc. 3rd Int. Conf. Learn. Represent. (ICLR)*, 2015, pp. 1–11.
- [127] A. Kurakin, I. Goodfellow, and S. Bengio, "Adversarial examples in the physical world," in *Proc. Workshop Track Int. Conf. Learn. Represent. (ICLR)*, 2017, pp. 1–14.
- [128] A. Madry, A. Makelov, L. Schmidt, D. Tsipras, and A. Vladu, "Towards deep learning models resistant to adversarial attacks," in *Proc. Int. Conf. Learn. Represent. (ICLR)*, 2018, pp. 1–28.
- [129] S.-M. Moosavi-Dezfooli, A. Fawzi, and P. Frossard, "DeepFool: A simple and accurate method to fool deep neural networks," in *Proc. IEEE Conf. Comput. Vis. Pattern Recognit. (CVPR)*, Jun. 2016, pp. 2574–2582.
- [130] N. Narodytska and S. P. Kasiviswanathan, "Simple black-box adversarial perturbations for deep networks," 2016, arXiv:1612.06299. [Online]. Available: <https://arxiv.org/abs/1612.06299>
- [131] J. Su, D. Vargas, and K. Sakurai, "One pixel attack for fooling deep neural networks," *IEEE Trans. Evol. Comput.*, vol. 23, no. 5, pp. 828–841, Oct. 2019.
- [132] W. Brendel, J. Rauber, and M. Bethge, "Decision-based adversarial attacks: Reliable attacks against black-box machine learning models," in *Proc. Int. Conf. Learn. Represent. (ICLR)*, 2018, pp. 1–12.
- [133] T. Huang, Y. Chen, B. Yao, B. Yang, X. Wang, and Y. Li, "Adversarial attacks on deep-learning-based radar range profile target recognition," *Inf. Sci.*, vol. 531, pp. 159–176, Aug. 2020.
- [134] T. Huang, Q. Zhang, J. Liu, R. Hou, X. Wang, and Y. Li, "Adversarial attacks on deep-learning-based SAR image target recognition," *J. Netw. Comput. Appl.*, vol. 162, Jul. 2020, Art. no. 102632.
- [135] B. Lewis, K. Cai, and C. Bullard, "Adversarial training on SAR images," *Proc. SPIE*, vol. 11394, pp. 83–90, Apr. 2020.
- [136] L. Wang, X. Wang, S. Ma, and Y. Zhang, "Universal adversarial perturbation of SAR images for deep learning based target classification," in *Proc. IEEE 4th Int. Conf. Electron. Technol. (ICET)*, May 2021, pp. 1272–1276.
- [137] S.-M. Moosavi-Dezfooli, A. Fawzi, O. Fawzi, and P. Frossard, "Universal adversarial perturbations," in *Proc. IEEE Conf. Comput. Vis. Pattern Recognit. (CVPR)*, Jul. 2017, pp. 86–94.
- [138] S. Wagner, C. Panati, and S. Bruggenwirth, "Fool the COOL—On the robustness of deep learning SAR ATR systems," in *Proc. IEEE Radar Conf. (RadarConf)*, May 2021, pp. 1–6.
- [139] J. Deng, W. Yi, K. Zeng, Q. Peng, and X. Yang, "Supervised learning based online filters for targets tracking using radar measurements," in *Proc. IEEE Radar Conf. (RadarConf)*, Sep. 2020, pp. 1–6.
- [140] C. Gao, J. Yan, S. Zhou, P. K. Varshney, and H. Liu, "Long short-term memory-based deep recurrent neural networks for target tracking," *Inf. Sci.*, vol. 502, pp. 279–296, Oct. 2019.
- [141] C. Gao, J. Yan, S. Zhou, B. Chen, and H. Liu, "Long short-term memory-based recurrent neural networks for nonlinear target tracking," *Signal Process.*, vol. 164, pp. 67–73, Nov. 2019.
- [142] J. Liu, Z. Wang, and M. Xu, "DeepMTT: A deep learning maneuvering target-tracking algorithm based on bidirectional LSTM network," *Inf. Fusion*, vol. 53, pp. 289–304, Jan. 2020.
- [143] W. Yu, H. Yu, J. Du, M. Zhang, and J. Liu, "DeepGTT: A general trajectory tracking deep learning algorithm based on dynamic law learning," *IET Radar, Sonar Navigat.*, vol. 15, no. 9, pp. 1125–1150, Sep. 2021.
- [144] Y. Shi, B. Jiu, J. Yan, H. Liu, and K. Li, "Data-driven simultaneous multibeam power allocation: When multiple targets tracking meets deep reinforcement learning," *IEEE Syst. J.*, vol. 15, no. 1, pp. 1264–1274, Mar. 2021.
- [145] A. Mendoza, A. Soto, and B. C. Flores, "Classification of radar jammer FM signals using a neural network," *Proc. SPIE*, vol. 10188, pp. 526–536, May 2017.
- [146] G. Shao, Y. Chen, and Y. Wei, "Convolutional neural network-based radar jamming signal classification with sufficient and limited samples," *IEEE Access*, vol. 8, pp. 80588–80598, 2020.
- [147] G. Shao, Y. Chen, and Y. Wei, "Deep fusion for radar jamming signal classification based on CNN," *IEEE Access*, vol. 8, pp. 117236–117244, 2020.
- [148] Q. Liu and W. Zhang, "Deep learning and recognition of radar jamming based on CNN," in *Proc. 12th Int. Symp. Comput. Intell. Design (ISCID)*, Dec. 2019, pp. 208–212.
- [149] Y. Xiao, J. Zhou, Y. Yu, and L. Guo, "Active jamming recognition based on bilinear EfficientNet and attention mechanism," *IET Radar, Sonar Navigat.*, vol. 15, no. 9, pp. 957–968, Sep. 2021.
- [150] M. Tan and Q. V. Le, "EfficientNet: Rethinking model scaling for convolutional neural networks," 2019, arXiv:1905.11946. [Online]. Available: <https://arxiv.org/abs/1905.11946>
- [151] Y. Junfei, L. Jingwen, S. Bing, and J. Yuming, "Barrage jamming detection and classification based on convolutional neural network for synthetic aperture radar," in *Proc. IEEE Int. Geosci. Remote Sens. Symp. (IGARSS)*, Jul. 2018, pp. 4583–4586.

- [152] W. Wenying, W. Yao, Z. Xuanxuan, Y. Hui, and W. Ruqi, "Classifying aircraft based on sparse recovery and deep-learning," *J. Eng.*, vol. 2019, no. 21, pp. 7464–7468, Nov. 2019.
- [153] L. Kang, J. Bo, L. Hongwei, and L. Siyuan, "Reinforcement learning based anti-jamming frequency hopping strategies design for cognitive radar," in *Proc. IEEE Int. Conf. Signal Process., Commun. Comput. (ICSPCC)*, Sep. 2018, pp. 1–5.
- [154] K. Li, B. Jiu, P. Wang, H. Liu, and Y. Shi, "Radar active antagonism through deep reinforcement learning: A way to address the challenge of mainlobe jamming," *Signal Process.*, vol. 186, Sep. 2021, Art. no. 108130.
- [155] S. Ak and S. Bruggenwirth, "Avoiding jammers: A reinforcement learning approach," in *Proc. IEEE Int. Radar Conf. (RADAR)*, Apr. 2020, pp. 321–326.
- [156] S.-J. Hong, Y.-G. Yi, J. Jo, and B.-S. Seo, "Classification of radar signals with convolutional neural networks," in *Proc. 10th Int. Conf. Ubiquitous Future Netw. (ICUFN)*, Jul. 2018, pp. 894–896.
- [157] G.-H. Lee, J. Jo, and C. H. Park, "Jamming prediction for radar signals using machine learning methods," *Secur. Commun. Netw.*, vol. 2020, pp. 1–9, Jan. 2020.
- [158] P. Sharma, K. K. Sarma, and N. E. Mastorakis, "Artificial intelligence aided electronic warfare systems-recent trends and evolving applications," *IEEE Access*, vol. 8, pp. 224761–224780, 2020.
- [159] D. Callaghan, J. Burger, and A. K. Mishra, "A machine learning approach to radar sea clutter suppression," in *Proc. IEEE Radar Conf. (RadarConf)*, May 2017, pp. 1222–1227.
- [160] M. Inggs, H. Griffiths, F. Fioranelli, M. Ritchie, and K. Woodbridge, "Multistatic radar: System requirements and experimental validation," in *Proc. Int. Radar Conf.*, Oct. 2014, pp. 1–6.
- [161] M. Pan, J. Chen, S. Wang, and Z. Dong, "A novel approach for marine small target detection based on deep learning," in *Proc. IEEE 4th Int. Conf. Signal Image Process. (ICSIP)*, Jul. 2019, pp. 395–399.
- [162] X. Chen, N. Su, Y. Huang, and J. Guan, "False-alarm-controllable radar detection for marine target based on multi features fusion via CNNs," *IEEE Sensors J.*, vol. 21, no. 7, pp. 9099–9111, Apr. 2021.
- [163] Q. An, Z. Pan, and H. You, "Ship detection in Gaofen-3 SAR images based on sea clutter distribution analysis and deep convolutional neural network," *Sensors*, vol. 18, no. 2, p. 334, Jan. 2018.
- [164] L. Ma, J. Wu, J. Zhang, Z. Wu, G. Jeon, Y. Zhang, and T. Wu, "Research on sea clutter reflectivity using deep learning model in industry 4.0," *IEEE Trans. Ind. Informat.*, vol. 16, no. 9, pp. 5929–5937, Sep. 2020.
- [165] L. Cifola and R. Harmann, "Target/clutter disentanglement using deep adversarial training on micro-Doppler signatures," in *Proc. 16th Eur. Radar Conf. (EuRAD)*, Oct. 2019, pp. 201–204.
- [166] P. Lepetit, C. Ly, L. Barthes, C. Mallet, N. Viltard, Y. Lemaitre, and L. Rottner, "Using deep learning for restoration of precipitation echoes in radar data," *IEEE Trans. Geosci. Remote Sens.*, early access, Feb. 19, 2021, doi: [10.1109/TGRS.2021.3052582](https://doi.org/10.1109/TGRS.2021.3052582).
- [167] Q. Zhang, Y. Shao, S. Guo, L. Sun, and W. Chen, "A novel method for sea clutter suppression and target detection via deep convolutional autoencoder," *Int. J. Signal Process.*, vol. 2, pp. 35–40, 2017.
- [168] S. Guo, Q. Zhang, Y. Shao, and W. Chen, "Sea clutter and target detection with deep neural networks," in *Proc. 2nd Int. Conf. Artif. Intell. Eng. Appl.*, Lancaster, PA, USA, 2017, pp. 316–326.
- [169] J. Zhao, J. Wu, X. Guo, J. Han, K. Yang, and H. Wang, "Prediction of radar sea clutter based on LSTM," *J. Ambient Intell. Hum. Comput.*, vol. 4, pp. 1–8, Sep. 2019.



ZHE GENG (Member, IEEE) received the dual B.S. degrees (*magna cum laude*) in electrical engineering from Florida International University (FIU), Miami, FL, USA, and Hebei University of Technology, Tianjin, China, in 2012, and the Ph.D. degree in electrical engineering from FIU, in 2018. From 2018 to 2019, she was a Research Scientist with Wright State University, Dayton, OH, USA. In December 2019, she joined the

College of Electronic and Information Engineering, Nanjing University of Aeronautics and Astronautics (NUAA), where she is currently an Associate Professor. She is the second author of *Radar Networks* (CRC Press, 2020). Her research interests include MIMO radar and joint radar-communications systems. She was a recipient of the FIU's most prestigious awards for entering doctoral students, the FIU Presidential Fellowship.



HE YAN received the B.S. degree from Jilin University, Changchun, China, in 2008, and the Ph.D. degree in communication and information system from The University of Chinese Academy of Sciences, Beijing, China, in 2013. From 2013 to 2014, he was an Engineer with the 14th Research Institute of China Electronics Technology Group Corporation (CETC-14), Nanjing, China. Since 2015, he has been an Associate Professor with the College of Electronic and Information Engineering, Nanjing University of Aeronautics and Astronautics (NUAA), Nanjing. His main research interests include synthetic aperture radar-ground moving target indication (SAR-GMTI), wide area surveillance-ground moving target indication (WAS-GMTI), video synthetic aperture radar-ground moving target indication (ViSAR-GMTI), and ocean current measurements based on spaceborne SAR.



JINDONG ZHANG was born in Nantong, China, in 1981. He received the B.S., M.S., and Ph.D. degrees in electronic engineering from Nanjing University of Science and Technology, Nanjing, China, in 2004, 2006, and 2010, respectively. In 2010, he joined the College of Electronic and Information Engineering, Nanjing University of Aeronautics and Astronautics, Nanjing, where he is currently an Assistant Professor. He developed a graduate level course on radar signal analysis and processing. His current research interests include cognitive radar and adaptive radar waveform design. He is a member of the Key Laboratory of Radar Imaging (Nanjing University of Aeronautics and Astronautics), Ministry of Education. In 2019, he received the Second Class Prize of The State Scientific and Technological Progress Award for radar systems development as a member of the Technical Team.



DAIYIN ZHU was born in Wuxi, China, in 1974. He received the B.S. degree in electronic engineering from Southeast University, Nanjing, China, in 1996, and the M.S. and Ph.D. degrees in electronics from Nanjing University of Aeronautics and Astronautics (NUAA), Nanjing, in 1998 and 2002, respectively. From 1998 to 1999, he was a Guest Scientist with the Institute of Radio Frequency Technology, German Aerospace Center (DLR), Cologne, Germany, where he worked in the field of SAR interferometry. In 1998, he joined the Department of Electronic Engineering, NUAA, where he is currently a Professor. He has developed algorithms for several operational airborne SAR systems. His current research interests include radar imaging algorithms, SAR ground moving target indication, SAR/ISAR autofocus techniques, and SAR interferometry.